2000

Characterization of Cosmic Microwave Background Temperature Fluctuations for Cosmological Topologies Specified by Topological Betti Numbers

Troy Gobble
Eastern Illinois University

THESIS/FIELD EXPERIENCE PAPER REPRODUCTION CERTIFICATE

TO: Graduate Degree Candidates (who have written formal theses)

SUBJECT: Permission to Reproduce Theses

The University Library is receiving a number of request from other institutions asking permission to reproduce dissertations for inclusion in their library holdings. Although no copyright laws are involved, we feel that professional courtesy demands that permission be obtained from the author before we allow these to be copied.

PLEASE SIGN ONE OF THE FOLLOWING STATEMENTS:

Booth Library of Eastern Illinois University has my permission to lend my thesis to a reputable college or university for the purpose of copying it for inclusion in that institution's library or research holdings.

8-3-00
Date

I respectfully request Booth Library of Eastern Illinois University **NOT** allow my thesis to be reproduced because:

_____

_____

_____

_____ _____

Author's Signature Date

Characterization of Cosmic Microwave Background Temperature Fluctuations for Cosmological Topologies Specified by Topological Betti Numbers

BY

TROY GOBBLE

THESIS

SUBMITTED IN PARTIAL FULFILLMENT OF THE REQUIREMENTS
FOR THE DEGREE OF

MASTER OF SCIENCE IN NATURAL SCIENCES

IN THE GRADUATE SCHOOL, EASTERN ILLINOIS UNIVERSITY
CHARLESTON, ILLINOIS

2000
YEAR

I HEREBY RECOMMEND THAT THIS THESIS BE ACCEPTED AS FULFILLING THIS PART OF THE GRADUATE DEGREE CITED ABOVE

August 3, 2000
DATE

August 3, 2000
DATE

Department of Physics
Master of Science in Natural Sciences
Physics Concentration
Thesis Acceptance

Title:
Characterization of Cosmic Microwave Background temperature fluctuations for cosmological topologies specified by topological Betti numbers

By
Mr. Troy Gobble

The undersigned Thesis Committee hereby recommend that this thesis Be accepted as fulfilling part of the Masters of Science in Natural Sciences in Physics degree program:

Date: July 26, 2000

Date: July 26, 2000

Date: July 26, 2000

Abstract

The cosmic microwave background explorer, COBE, and the Balloon Observations of Millimetric Extragalactic Radiation and Geophysics, BOOMERanG, have collected data from the universe and detected relic anisotropies indicative of one of the earliest events of the universe, decoupling. Hidden in the correlation between these temperature fluctuations is the signature of the global shape, or topology, of the early universe. It is possible to calculate the temperature fluctuations as due to primeval adiabatic density temperature fluctuations from the Sachs-Wolfe effect, which contains a topological term. Here we investigate some of the spaces and how they affect the microwave background.

A large class of spaces can be understood with some tools of topology associated with the way curves and volumes divide a space. The three tools of interest are the Euler Characteristic, the Betti numbers and fundamental domains. We intend to demonstrate the relationship between topology and anisotropy by creating a general equation that contains a topological term based on a topological invariant, the Betti Numbers of a manifold, and a term based on the temperature fluctuations.

We will also extend the work of Silk on classifying the finite flat spaces through the use of a new three-dimensional plotting

technique. These graphs demonstrate the inadequacy of the current CMB data's topological predictive properties. As many shapes can produce the observed peaks. We will also extend the work of Inoue on classifying compact hyperbolic manifolds in two ways. First we demonstrate that the compact hyperbolic eigenmodes can be represented by a ${}_pF_q$ function, and do not need to be calculated individually. Secondly, we extend the power spectrum plot the high angular resolution, large l, and compare compact hyperbolic manifolds to the observed peak in the BOOMERanG data at $l = 200$.

Dedication

For my Mom and Dad,

I love you both.

Acknowledgements

I would like to thank the members of my committee, Dr. James C. Conwell and Dr. James A. McGaughey, for taking time out of their schedules to read and evaluate my thesis. I would also like to thank Sharon Nichols for her continuous support.

Most of all, I would like to extend my deepest appreciation to my advisor, Dr. Keith Andrew, without whom this project would have never come to completion.

Table of Contents

List of Figures

List of Figures

List of Tables

List of Appendices

Introduction

What is the shape of the space? What is the shape of the universe we live in? These questions are very difficult to even think about. The spatial universe is three dimensional and hard to comprehend because it is just so big. The solution to this problem is very similar to a problem mankind has already solved, What is the shape of the Earth? Let's start there. Centuries ago, it was common to believe that the Earth was flat. This notion seems silly today, but look out the window, when the surface of the Earth is examined in small pieces it seems very flat. Early people wondered if the Earth went on forever, or if there was an edge. If it did have an edge, could they fall off? It is now obvious that the surface of the Earth is not flat, but nearly a sphere. It does not go on forever, but it does not have any edges, or boundaries. Theoretically, one could take a trip all the way around the Earth, thousands of miles and come back to the starting place. Could this happen in our universe, also? Could a spaceship be flown in a straight line away from the Earth and eventually find itself right back where it started? Would we even be able to tell we were back on the Earth, or would it look different to us after the trip? By combining what we know about the history of the universe, specifically the Big Bang, and topology, the study of shapes, the universe might take shape right before our eyes.

The Early History of Cosmological Topology

Is the universe finite or infinite, simply or multiply connected, orientable or not? Does it have holes? What is its global shape? These questions have been pondered for thousands of years. Many believed the answers to these questions were contained in Einstein's theory of General Relativity. This is not the case. General relativity deals only with local geometrical properties of the universe, such as curvature. It does not contain global information such as topology. (1)

At the beginning of the Twentieth century, many finite spaces without boundaries had been discovered and classified; many of these spaces were of non-trivial topology. On a finite space without a boundary, light could travel completely around the universe and return to where it began, like a jet plane flying around the earth. This idea was very exciting. Imagine looking into the night sky and seeing light from our very sun coming back to us as starlight. Schwarzschild remarked [2] in 1900: "One could imagine that as a result of enormously extended astronomical experience, the entire universe consists of countless identical copies of our Milky Way, that the infinite space can be partitioned into cubes each containing an exactly identical copy of our Milky Way. Would we really cling on to the assumption of infinitely many identical repetitions of the same world?" Schwarzschild's imaginary infinite universe could also be

described as a universe shaped as a three dimensional torus, or simply one Milky Way cube that is connected such that by exiting one side of the cube one will enter the other side.

After Einstein's 1915 discovery of General Relativity, many believed the answers to these cosmological questions were contained in Einstein's new equations. This would not prove to be the case. General relativity deals only with local geometrical properties of the universe, such as curvature. Since Einstein's equations are coupled nonlinear partial differential equations, they describe only local geometrical properties of spacetime. They allow us to calculate the components of the curvature tensor at any non-singular point in spacetime. Einstein's equations do not fix the global structure of spacetime. More than one (and sometimes an infinite set of) topologically distinct global shapes correspond to any given metric solution of the field equations (1).

Einstein believed that the universe must be finite and chose a sphere as the shape of the universe for his static cosmological solution. In fact, he does not mention any other possible alternatives to the spherical case. In a letter to Weyl, Einstein writes: "Nevertheless I have like an obscure feeling which leads me to prefer the spherical model. I have a feeling that manifolds in which any closed curve can be continuously contracted to a point are the

simplest ones" [3] His choice of the sphere does not seem to be based on physical reasoning.

Freidman and Lemaitre discovered non-static cosmological solutions that are now referred to as the big bang theory of the creation of the universe. This meant the universe had a beginning, and was not infinitely old. They also worked on the curvature of the universe, and they realized the cosmological constant's sign gave important information about the type of three dimensional space we live on. A positive curvature would imply spherical, a negative curvature would imply a hyperbolic space, and a zero curvature would describe Euclidian space. Freidman was also able to show that one solution to Einstein's equations could describe several topological spaces.

The development of the big bang theory and our understanding of the events that followed have put significant constraints on possible shapes of the universe. A great deal of work has been done on flat models of the universe [4,5,6,7] and the study of compact hyperbolic models has begun[8,9,10]. The angular resolution with which we study the sky has gotten smaller and smaller and this improved data has supplied even greater constraints to the global shape. How these topics are related will be explored in the following chapters.

THE BEGINNING

It is now generally accepted that the future of the universe must have been determined in the first few moments of the Big Bang. In the last twenty years, a convincing theory of the origin and evolution of the universe has developed, known as the standard cosmological model. Although there are other models, such as the Steady State theory, this is the most widely accepted. Imagine going back to the earliest of times, as close to the Big Bang as possible, and following the chain of events as the universe cools, expands, and takes shape.

The first time we have knowledge of is the Planck era 10^{-43} seconds after the Big Bang. Before this time, it is widely believed that the four fundamental forces (gravity, electromagnetism, strong and weak) were unified, or acted as one force. As the universe expanded, it also cooled. This cooling caused the four forces to separate one by one from the combined force. This separating out is analogous to the phase changes a substance undergoes as it cools. Water can cool from 90° C to 10° C and its basic form will not change. When it reaches 0° C, it undergoes a phase change and will begin to change form. The forces stayed unified until a certain temperature, about 10^{32} K, and then gravity separated from the other forces. This period is known as the Grand Unified Era, or GUT, and there was no difference between quarks and leptons. At 10^{-35} seconds after the Big Bang, the temperature of the universe was 10^{27} K and the strong force

"condensed out." The universe was now filled with quarks and many different types of leptons. At about this time the universe underwent inflation, growing in size by a factor of up to 10^{50}. The size of the universe changed from smaller than a proton, to larger than a grapefruit.

At 10^{-12} seconds after the Big Bang, the universe entered what is known as the Hadron era; because the hadrons were the dominant form of matter. The last "force phase change" took place as the weak force and the electromagnetic force developed separate qualities. Quarks began to combine in threes to form protons and neutrons, but the temperature was still high enough that these baryons would collide and break back into quarks. The universe continued to expand and cool, when the temperature reached about 10^{13}K, baryonic collisions were not energetic enough to smash themselves apart. The number of protons and neutrons stabilized and all quarks were now combined inside them. Lighter particles dominated the universe, like electrons, positrons, neutrinos and photons. In the next few seconds, electrons went through a similar creation and annihilation process as the hadrons, first they had enough energy to collide and break apart, but when the temperature of the universe went below 10^{10} K, electrons and positrons lacked the energy to break apart and their number stabilized.

This marked the beginning of the radiation dominated era in the early universe. Photons and neutrinos contained most of the energy in the universe, and would for the next 300,000 years. At this point the universe was at a temperature of about 3000 K. Nuclear fusion had taken place in the first hour of the universe, creating deuterium, helium and possibly even lithium nuclei, but up until this point the universe had been too hot for electrons to be captured by these bare nuclei. The photons in the universe had too much energy to allow the electrons to bind to form atoms. About 300,000 years after the big bang, the energy of the photons dropped enough to allow atoms to form. This period is known as the Era of Recombination. Prior to this time period, the universe would have looked like the hot, glowing, opaque gas (like the sun) everywhere. The entire universe was a plasma. After recombination, hydrogen atoms would no longer interact with the lower energy photons. The temperature of the radiation and the matter had up until this point been the same. Now that they interacted much less frequently, and their temperatures would begin to diverge. Photons that had been previously bouncing from particle to particle could now travel freely though space. Suddenly, the universe was transparent. All observations made with radio telescopes can see back only to the moment of transparency. No matter how good the technology becomes, it is impossible to use electromagnetic waves to see farther in the past.

Parameters of the Universe

In order to make predictions about the shape of the universe, it is very important to understand the physical limitations of the universe. These parameters will determine almost everything we know about the universe. The parameters are: the density of the baryons in the universe, the cosmological constant, the Hubble constant, the age of the universe, the temperature of the cosmic microwave background, and the density of the cold dark matter in the universe.

The Hubble constant, developed by Edwin Hubble in 1919, measures the expansion rate of the universe. This "constant" has changed over time, so it is common to refer to H_o the expansion rate of the universe right now. The value of H_o is generally thought to be 65 km/s/Mpc ± 15 km/s/Mpc. The Hubble constant is very useful in helping to produce dimensionless density parameter, Ω, using the following equation

$$\Omega = 8\pi\rho G/3H^2 \qquad (1)$$

where ρ is the density and G is the gravitational constant. If $\Omega > 1$, the density of matter in the universe is sufficient for expansion to be reversed (sometimes called the Big Crunch). If $\Omega = 1$, the universe will expand at a slower and slower rate. If $\Omega < 1$, the expansion will

continue forever and the universe will become colder (commonly called the Big Chill).

The density of baryons, protons and neutrons, in the universe is $\Omega_B = .03 \pm 20\%$. This value is very small, and if the universe were only made of baryons, the Big Chill would be inevitable. There are other things that must be considered when finding the total density of the universe. Remember that not all matter in the universe is glowing, and is therefore very difficult to observe. This cold dark matter is thought to have a density in the following range, $\Omega_{CDM} = 0 - 0.97$. The great uncertainty of this number is because it is hard to detect. Another number that helps determine the total density of the universe is the cosmological constant, Λ. This is the quantity that Einstein created in 1917 so that General Relativity would predict a static universe. Although the universe is now known to be expanding, the constant has remained, and now represents the energy density of a vacuum. The common prediction of this value is between $0 < \Lambda < 0.7$.

The parameter that is most accurately known is the temperature of the universe. It is measured from the cosmic microwave background radiation that permeates all of space. The accepted value is $T = 2.728K \pm 0.1\%$. The last parameter that ios important is the age of the universe. The current prediction about the age of the universe is based on the Hubble constant and the

density parameters. It is estimated to be about 12 billion years ± 2 billion years since the Big Bang.

It is amazing to think we have such great knowledge of the vast universe, but it is important to note the great uncertainty in these parameters. NASA is planning to launch two satellites in the next decade that should reduce the uncertainty of these numbers to less than 1%.

Cosmic Microwave Background Radiation

This point marks the end of the Radiation-dominated era of the universe and begins the Matter-dominated era of the universe. The radiation, freed from constant interaction with the matter, continues to expand with the universe. This expansion of the universe has caused the radiation to be stretched, or redshifted, by a factor of $z = 1000$. Because of this, the photons have a wavelength of 10 cm and are now observable only in the microwave range of the electromagnetic spectrum. As the universe cooled, the radiation cooled down from a recombination temperature of about 3000 K to the 2.726 K observed today. Because this radiation existed everywhere in the early universe, it is detectable at approximately the same intensity from all parts of the sky. The radiation is cosmic, existing everywhere in space. There are about 400 photons of this radiation moving at the speed of light through every square centimeter of the universe at all times. It has filled all of space at all times since recombination. The radiation is given a special name, the cosmic microwave backgound (CMB) radiation. The discovery and understanding of the cosmic microwave background in 1964 has provided a great amount of new information about the universe. It has provided data about the temperature of the early universe,

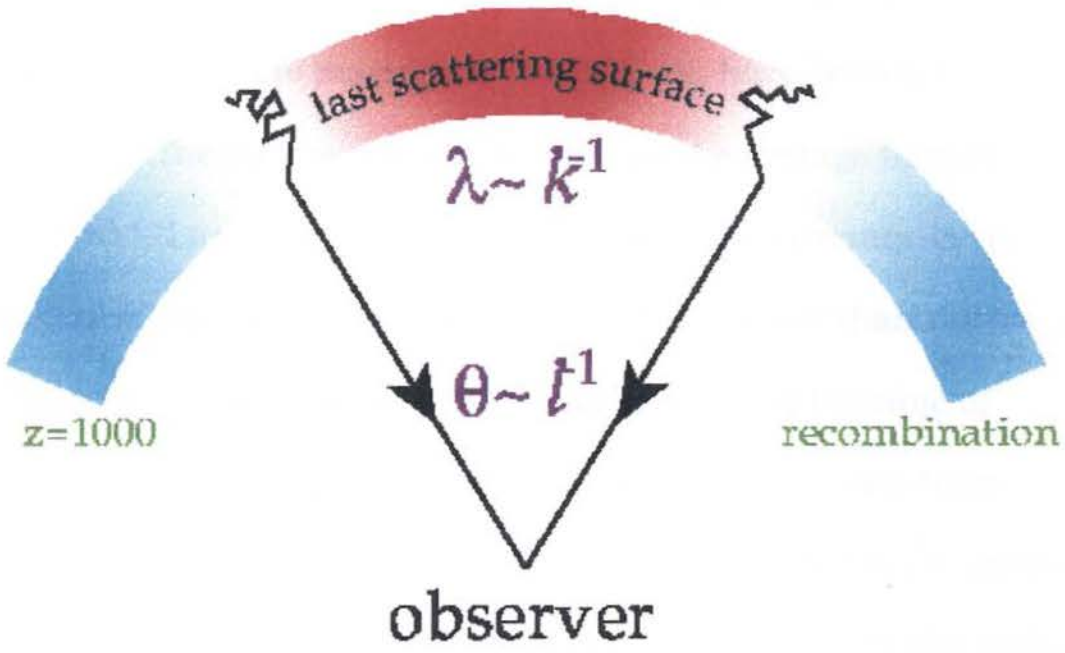

Figure 1: Photons Traveling from the Recombination Period [12]

helped establish a time frame for the big bang, and it allowed astronomers to look back in time and conclude the universe was very homogenous and isotropic.

Initial measurements of the cosmic microwave background proved difficult because the Earth's atmosphere is almost completely opaque to microwave frequencies. Good observations can only be made from balloons at very high altitudes, or, better yet, on orbiting spacecraft. The most accurate map of our entire sky was collected by the Cosmic Background Explorer (COBE) satellite, which was launched in 1989.

All early predictions about the COBE data assumed that COBE would show that the CMB was smooth everywhere. The average temperature of the CMB has been accurately measured to 2.726 K,

but it is not the same everywhere. Very small temperature fluctuations, on the magnitude of ± 100 μK, have been detected (see Figure 2). The blue areas are cooler than the average temperature by about 10^{-4} K and the red areas are warmer than average by 10^{-4} K. The cooler regions would have been slightly denser than the warmer regions in the early universe. This means that at the time of recombination, the matter and radiation could not have been completely uniform. The density of the matter in the early universe was smooth, but not perfectly smooth. Little bumps in the matter distribution were like seeds for the formation of the large-scale structure of the universe.

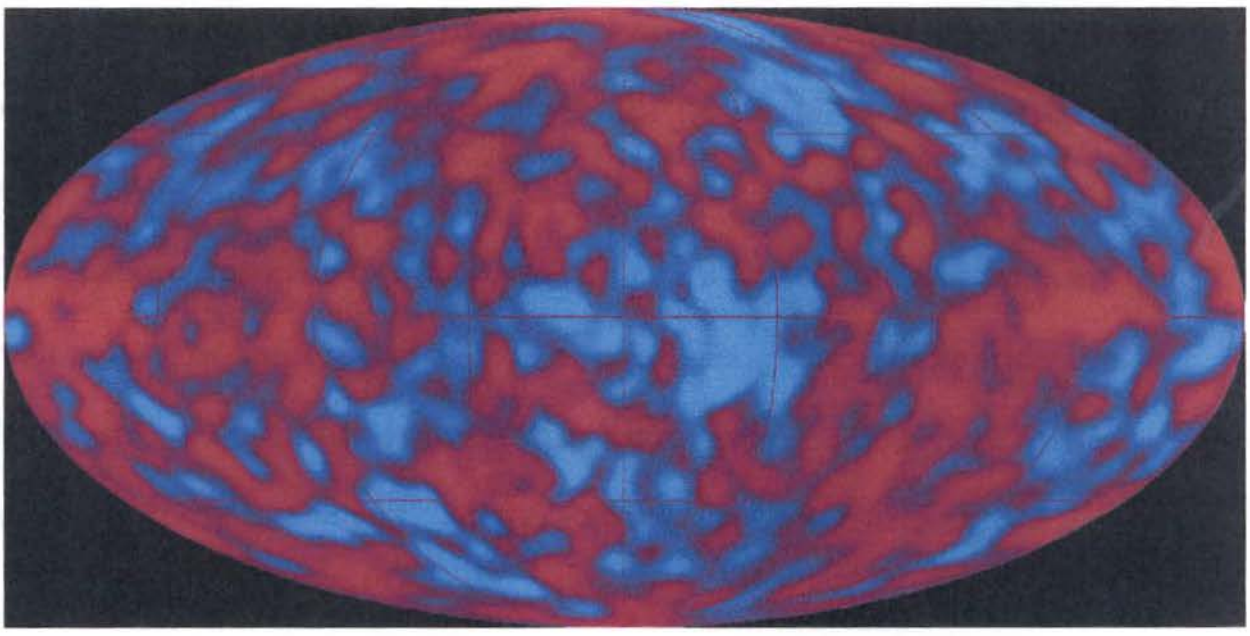

FIGURE 2: COBE map of temperature anisotropies in the CMB.[11]

These denser areas, or clusters of matter, could have evolved into the large clusters of matter (galaxies) in today's universe. The COBE data biggest shortcoming is the angular resolution of its measurement,

about 7°. Substantial clusters of galaxies can fit into such a large measurement.

An interesting effect occurs because of the cosmological horizon. Large chunks of matter will not begin to fall towards a wrinkle, or gravitational well, until the wrinkle reaches the horizon of the matter. Before that, the matter does not feel the gravitational effects. COBE does reveal the large scale wrinkles in the early universe before matter has had enough time to collect in the cooler regions. Examining widely separated angles from the COBE data only shows the primordial wrinkles because the distances between the wrinkles are too great for matter to have begun to feel gravity.

When scales smaller than the horizon are examined the process of structure formation can be observed. The small-scale fluctuations are actually sound waves in the early photon baryon fluid. Gravitation squeezes the fluid together and the radiation pressure resists it. The fluid heats as it is compressed, when it expands the fluid gets cooler. Sound waves in radiation can be observed as hot and cold spots in the sky. Acoustic oscillations are created

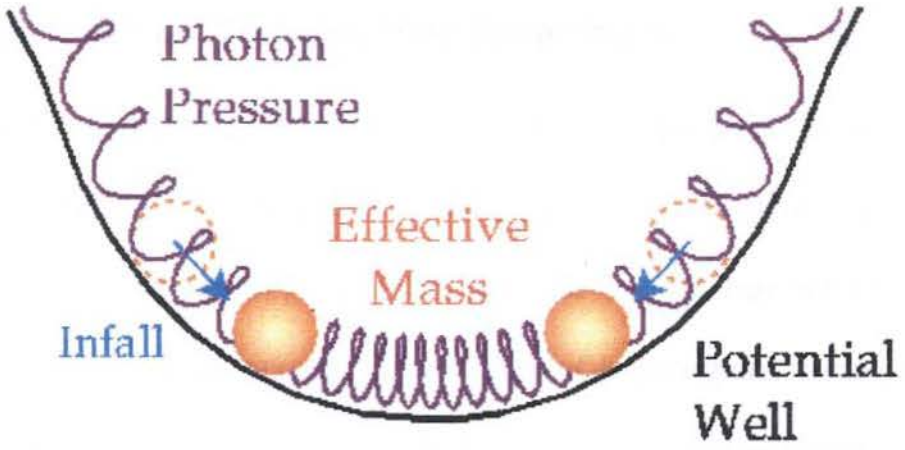

Figure 3: Spring model of Acoustic Oscillations[12]

as the fluid settles into the gravitational wells, or large scale cold spots. The shorter the wavelength, or back and forth motion of the matter, the faster the fluid oscillates. (12) These oscillations produced the cosmic microwave background fluctuations that have been observed today. Because the distances between the hot and cold spots are smaller than the horizon, matter will have collected in the gravitational potential wells, creating structures that are observable today.

Topology Part 1: Topological Invariants

A part of Topology deals with the general properties associated with the classification of all possible spatial shapes. The topology of a space consists of those properties that do not change when a surface is smoothly deformed. Examples of topological invariants include the Euler Characteristic, Betti number, connectivity, orientability, total curvature of the surface, and the number of holes and knots contained by the surface. The geometry of a space consists of the set of objects invariant under the action of symmetry. Examples of geometric properties are area, distance, and angle measure. The geometry of a basketball changes when you blow it up from completely flat to sphere shaped. The size of the basketball changes, the surface area and volume increase and an angle drawn on the completely deflated basketball will become larger when the basketball is inflated. The inflation does not change the topology of the basketball. The universe has expanded in the same fashion as the inflated basketball. The data that mat be used to determine the shape of the universe is the Cosmic Microwave Background radiation given off billions of years ago. The geometry of the universe has most certainly changed as it has expanded during this time, but the topology will have stayed the same.

It will be important to differentiate between local geometry and global topology. Local geometry are those properties observable in a

infinitesimally small region of the surface, while global topology refers to the surface as a whole. The sphere and the cube have the same global topologies, but their local geometry is different.

There are many properties that must be considered when discussing the topology of an object. A surface is **homogeneous** if the local geometry is constant across the entire surface. A sphere or a plane is homogeneous, but a torus in not. Another important property of surfaces is whether it is **bounded**, or has an edge. A plane has no edges, but putting a hole in it will give it an boundary. Surfaces may also be classified as **finite** or infinite. A finite surface can be enclosed; an infinite surface goes on forever. While there are no boundaries on a sphere, it is finite. A surface is **closed** if it has no edges and is finite. The number of holes, or handles, in a surface is called the **genus** of the surface.

In 1750, Leonhard Euler published a paper that invented the mathematics of topology. In this paper, he develops a fundamental value for classifying spaces called the Euler Characteristic. The Euler Characteristic, χ, of a polyhedral surface is found by counting the vertices, faces and edges of the polyhedron and using the following formula:

$$\mathbf{V}\text{ertices} - \mathbf{E}\text{dges} + \mathbf{F}\text{aces} = \chi \qquad (1)$$

To find the Euler characteristic of a two dimensional square, consider the following diagram:

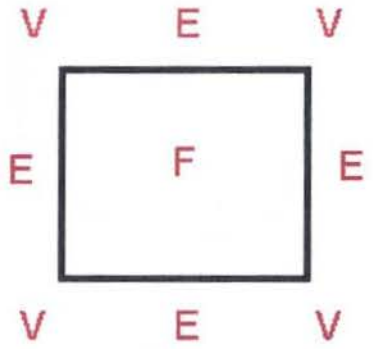

Number of Vertices = 4
Number of Edges = 4
Number of Faces = 1

$$\chi = 4 - 4 + 1 = 1$$

The Euler Characteristic of a square is 1.

Figure 4 : Euler Characteristic of a Square

To find the Euler Characteristic of a circle, it is helpful to break the circle up into smaller sections, or tiles. The number or size of the tiles can be chosen arbitrarily, which will of course change the number of vertices, edges and faces, but the same Euler constant will always be reached. Dividing a shape into smaller non-overlapping local sections, or triangulating the surface, will become very useful as the shapes become more complicated.

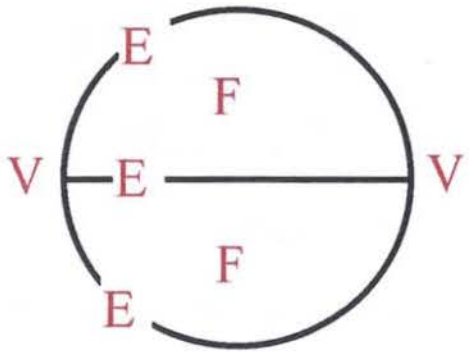

Number of Vertices = 2
Number of Edges = 3
Number of Faces = 2

$$\chi = 2 - 3 + 2 = 1$$

The Euler Characteristic of a circle is 1.

Figure 5 : Euler Characteristic of a Circle with Two Tiles

CIRCLE WITH 3 TILES

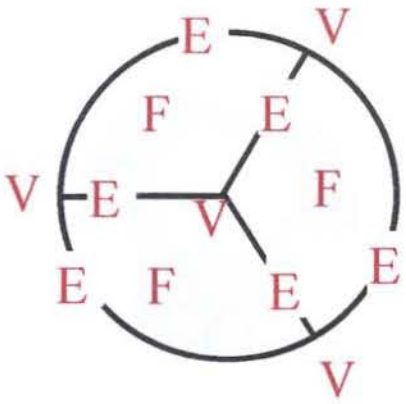

Number of Vertices = 4
Number of Edges = 6
Number of Faces = 3

$$\chi = 4 - 6 + 3 = 1$$

Again, the Euler Characteristic of a circle is 1.

Figure 6 : Euler Characteristic of a Circle with Three Tiles

Topologically, the circle is the same as a square, which is easy to visualize, just stretch the edges of the circle until it is in the form of a square. Deformation does not change topological properties.

The method of determining the Euler Characteristic remains the same for shapes in three dimensions or more. To find the Euler characteristic of a two dimensional square cube, consider Figure 7:

CUBE

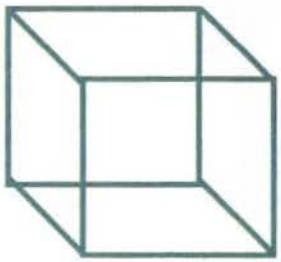

Number of Vertices = 8
Number of Edges = 12
Number of Faces = 6

$$\chi = 8 - 12 + 6 = 2$$

The Euler Characteristic of a cube is 2.

Figure 7 : Euler Characteristic of a Cube

The Euler Characteristic of this complicated polyhedron also has a value of 2 .

POLYHEDRON

Number of Vertices = 48
Number of Edges = 72
Number of Faces = 26

$$\chi = 48 - 72 + 26 = 2$$

The Euler Characteristic of this shape is also 2.

Figure 8 : Euler Characteristic of a Polyhedron

The cube and this polyhedron are topologically equivalent. Actually, the Euler Characteristic is an invariant for all simple polyhedra. Using the polyhedron from the previous example, it is easy to demonstrate, in Figure 6, that a sphere is topologically equivalent to the polyhedron by deformation. Because they are topologically the same, the Euler Characteristic of the sphere must also be 2.

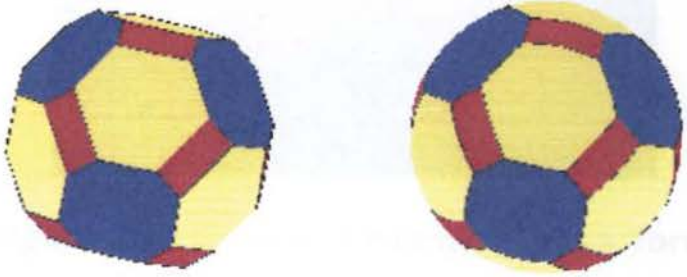

Figure 9 : Deformation of a Polyhedron into a Sphere

Euler incorrectly predicted that all polyhedra would have an Euler Characteristic of 2. Antoine-Jean Lhuilier noticed this was not correct for a simple open-ended cylinder, or any solids

CYLINDER

Number of Vertices = 0
Number of Edges = 2
Number of Faces = 2

$$\chi = 0 - 2 + 2 = 0$$

The Euler Characteristic of a cylinder is 0.

Figure 10 : Euler Characteristic of a Cylinder

with holes in them. In 1813, Lhuilier published a paper introducing the number of holes, or the genus, into the Euler equation.

$$\chi = 2 - 2g \qquad (2)$$

Where g represents the number of holes in an object. A more complicated surface with one hole is called a torus, or a donut shape. Imagine taking the ends of the simple cylinder and

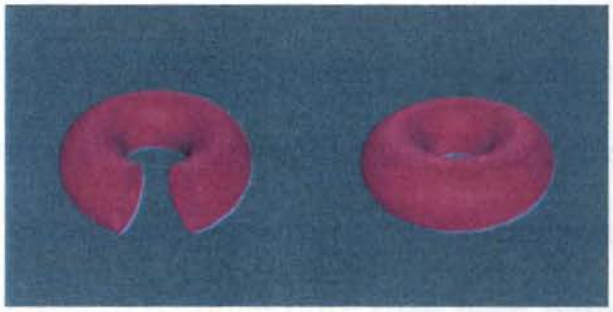

Figure 11 : Cylinder Deformed into a Torus

wrapping them around until they fit together (**Figure 11**). This deformation of the cylinder should not change its topological properties, therefore, the Euler Characteristic of a torus should be 0. To find the Euler characteristic of a torus and a two-torus, consider Figure 12 and Figure 13:

TORUS

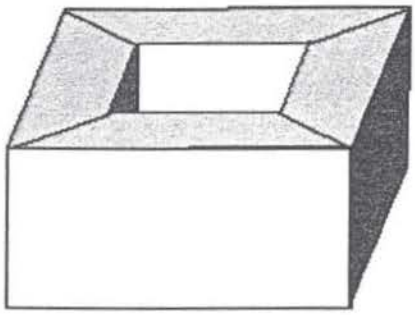

Number of Vertices = 16
Number of Edges = 32
Number of Faces = 16

$$\chi = 16 - 32 + 16 = 0$$

The Euler Characteristic of a torus is 0 .

Figure 12 : The Euler Characteristic of a Torus

TWO-TORUS

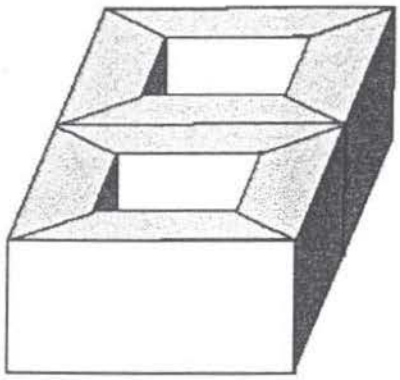

Number of Vertices = 28
Number of Edges = 60
Number of Faces = 30

$$\chi = 28 - 60 + 30 = -2$$

The Euler Characteristic of a two- torus is -2.

Figure 13 : The Euler Characteristic of a two-torus

It is important to note that the shape of the object, the size of the hole, or the shape of the hole does not affect the topology. A donut is topologically equivalent to a coffee cup; they both have one hole, or a genus of one.

Finally, surfaces may be **orientable or non-orientable**. If an object completes one trip around the surface and returns to the starting point reversed, like a mirror image, the surface is non-orientable. A non-orientable surface is commonly referred to as

having a twist or a crosscap. Mobius strips and Klein Bottles are non-orientable, an example of a klein bottle is shown below in figure 14. If all paths around the surface return and the traveler unchanged, the surface is orientable.

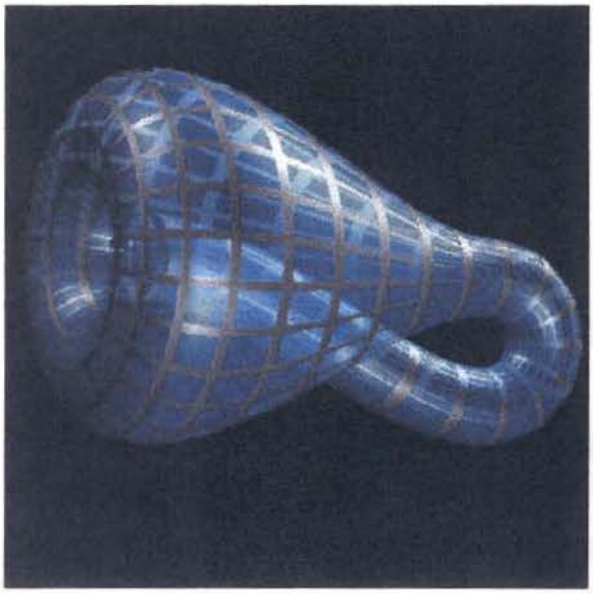

Figure 14: Klein Bottle

The sphere and torus are orientable. Orientable surfaces also have unique cross products. In a nonorientable surface, two people living on the same space might define the right hand rule in different directions. An orientable space could be defined as a space where all observers agree on the direction of the right hand rule. Orientability is a property of shapes that was not included in Euler's treatment of topological invariants, but it is included in a classification system developed by Betti in the 1800's.

Betti numbers are topological numbers that only depend upon the overall global topology of the manifold. Betti numbers can be used to classify a large class of differentiable metric spaces. Any linear combination of Betti numbers is also a topological invariant, and the most important of these is the alternating sum, which gives the Euler Characteristic in any dimension[15].

$$\chi(M) = \sum_i (-1)^i \beta_i \tag{3}$$

β_0 represents the number of connected components of any space, M, in N dimensions. β_0 must equal 1 when discussing the shape of the universe, another unconnected piece would not be detectable. If M is compact and orientable, then the Betti numbers are symmetric, that is for any pth Betti number, β_p,

$$\beta_p = \beta_{N-p}. \tag{4}$$

This is known as the Poincare' duality. Because of this, all β_N of orientable surfaces must also be equal to one. Moreover, if M is simply connected, then $\beta_p = 0$, where $0 < p < N$.

The Betti numbers for a two dimensional sphere, S_2, are

$$\beta_0 = 1, \beta_1 = 0, \beta_2 = 1 \tag{5}$$

Which gives an Euler Characteristic of

$$\chi(S_2) = 1 - 0 + 1 = 2 \tag{6}$$

The genus, or number of holes, of a surface is reflected in β_1. Each hole or handle provides two ways in which the surface can be divided up in to independent cycles. Another way to think about the cycles is to imagine a circle drawn on the shape. Any place the circle could not contract to a point but instead gets stuck around a hole counts as a cycle. This method works for any N dimensional space, where the shape being contracted is of any dimension less than or equal to N-1. Neither of the orange circles in Figure 16 will be able to contract to a point because of the hole in the torus, thus a β_1 of 2 cycles.

Figure 16: Number of independent cycles on a torus

Thus $\beta_1 = 2g$, where g is the genus of the surface. A two dimensional torus can be cut into cycles in two ways, it has $\beta_1 = 2$, and it has genus, g=1. The Betti numbers for a two dimensional torus, T_2, are:

$$\beta_0 = 1, \beta_1 = 2, \beta_2 = 1 \tag{7}$$

The Euler Characteristic is found to be

$$\chi(T_2) = 1 - 2 + 1 = 0 \tag{8}$$

Cycles on a sphere can always be collapsed down to a singular point. In other words, no sphere of any dimension, S_N, has a hole. So the Betti numbers for any n-dimensional sphere go as

$$\beta_0 = \beta_N = 1, \beta_p = 0 \quad (9)$$

The Euler Characteristic is therefore

$$\chi(S_N) = 0 \text{ if N is odd,} \quad (10)$$

$$\chi(S_N) = 2 \text{ if N is even.} \quad (11)$$

Table 1 gives the Betti numbers for all two dimensional spaces and Table 2 gives the Betti numbers for selected three dimensional spaces.

Table 1: Betti Numbers of Two Dimensional Spaces

Name	Symbol	g	b	c	β_0	β_1	β_2
Sphere	S^2	0	0	0	1	0	1
Torus	T^2	1	0	0	1	2	1
Plane	E^2	0	0	0	1	0	1
Disk	D^2	0	1	0	1	1	1
Projective Planes	P^2	0	1	1	1	1	0
Klein Bottle	K^2	1	0	1	1	2	0
Mobius Strip	M^2	0	0	2	1	1	0

Table 2: Betti Numbers of Three Dimensional Spaces

Symbol		β_0	β_1	β_2	β_3
S^3		**1**	**0**	**0**	**1**
T^3	**T^2xS^1**	**1**	**3**	**3**	**1**
S^2xS^1		**1**	**1**	**1**	**1**

Topological Sums

Topology also presents rules for the adding spaces together to find their sum or multiplying spaces to find their product. This is useful here because the universe may not be a simple shape, it is more likely to be very complicated. To develop a shape that could describe the universe may require combining many simple spaces.

Consider any two spaces in the same number of dimensions, S^1 and S^2. Each of these spaces can be identified by their Euler Characteristics, χ_1 and χ_2. Each shape will also have a genus, or number of holes, g_1 and g_2. The Euler sum of the two topological spaces is given by the following equation [14]:

$$\chi (g_1) + \chi (g_2) = \chi (g_1 + g_2) + \chi (0) \quad (12)$$

The sum of the spaces gives two new shapes, $\chi (g_1 + g_2) + \chi (0)$.

$\chi (0) = 2$ is a space with a genus of zero, or an object with no holes. This is the topological equivalent of a sphere. The other shape formed will simply have the total number of holes of the original two shapes. A torus $\chi (1) = 0$, added to a torus $\chi (1) = 0$ will give:

$$\chi (1) + \chi (1) = \chi (g_1 + g_2) + \chi (0) \quad (13)$$

$$0 + 0 = \chi (g_1 + g_2) + 2 \quad (14)$$

$$\chi (g_1 + g_2) = -2 \qquad (15)$$

An object with $\chi = -2$ is a two-torus, T^2. Why would a torus plus a torus not equal just the two torus? When adding spaces, the entire surface of the two spaces must continue to exist after the addition. Consider two separate torodial, T^2, spaces each with g=1 and $\chi = 0$. Imagine placing these two tori together so they only came into contact at one point on each surface. When the two spaces are added, these two points would be lost creating the connection between the two. Points on the spaces cannot vanish, so this is not an accurate representation of how the spaces combine. Consider the same two tori. Distort each space so a small hemisphere protrudes from the space but does not tear the space (figure 17).

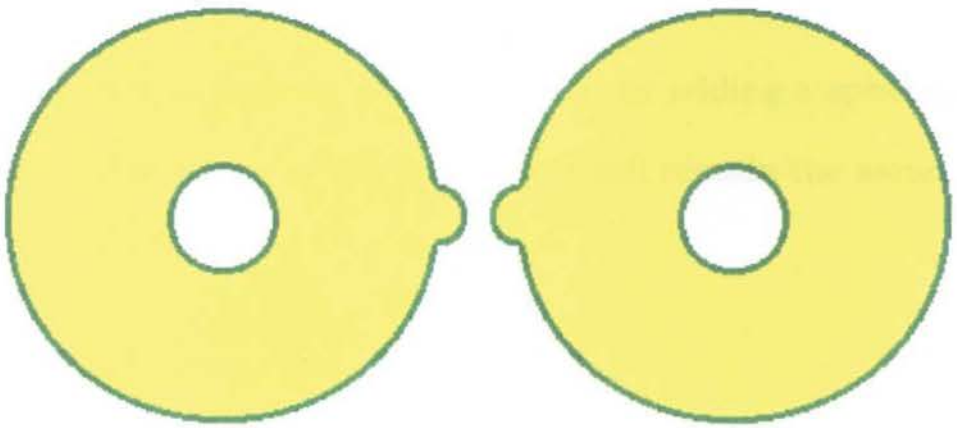

Figure 17: Adding two tori, T_2

Cut out the hole in each space leaving a hole in each torus and two separate hemispheres. Combine the two tori along the open hole to create a smooth seam. This is the combined space with $g = g_1 + g_2$.

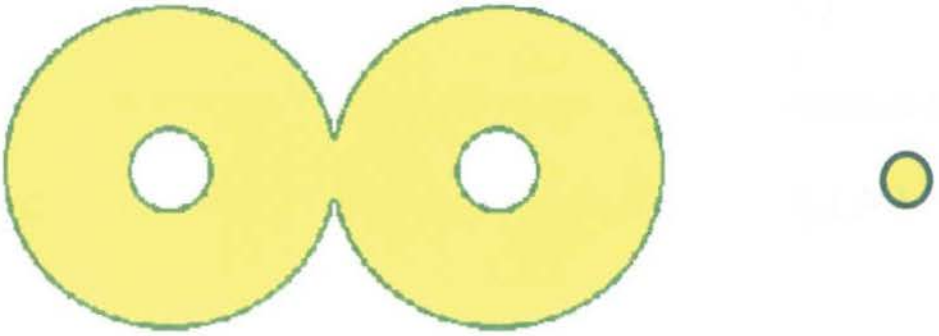

Figure 18: The sum of two tori, T^2

Also combine the two hemispheres together to form a sphere with g = 0. So the general form of the equation for a new space formed by addition is

$$\chi (g_1 + g_2) = \chi (g_1) + \chi (g_2) - \chi (0) \qquad (16)$$

It is simple to note from this equation that by adding a sphere, S^2, to any space the topology of the two objects will remain the same.

Multiplication of Spaces

Recall the formula for a product manifold in terms of the Euler Characteristic:

$$\chi(M \times N) = \chi(M) \times \chi(N) \tag{17}$$

If this is written in terms of Betti numbers it becomes [15]:

$$\beta_k(M \times N) = \sum_{p+q=k} \beta_p(M) \times \beta_q(N) \tag{18}$$

These are called the Kunneth formulas for product manifolds.

It is instructive here to construct some model spaces. To find the product of two circles, S^1, using the Euler Characteristic:

$$\chi(S^1 \times S^1) = \chi(S^1) \times \chi(S^1) = 0 \times 0 = 0 \tag{19}$$

The Betti numbers can also be used to develop a product.

$$\beta_k(S^1 \times S^1) = \sum_{p+q=k} \beta_p(S^1) \times \beta_q(S^1) \tag{20}$$

$$\beta_0(S^1 \times S^1) = \beta_0(S^1) \times \beta_0(S^1) = 1 \times 1 = 1 \tag{21}$$

$$\beta_1(S^1 \times S^1) = \beta_1(S^1) \times \beta_0(S^1) + \beta_0(S^1) \times \beta_1(S^1) = 1 + 1 = 2 \tag{22}$$

$$\beta_2(S^1 \times S^1) = \beta_1(S^1) \times \beta_1(S^1) = 1 \times 1 = 1 \tag{23}$$

A shape with χ=0, and $\beta_0 = 1$, $\beta_1 = 2$, $\beta_2 = 1$, is a torus, T^2.

The product of 2 tori, T^2, can be shown to be a four dimensional torus, T^4. It is simple to show that the Kunneth relations for the product yield [15]:

$$T^4:\begin{cases}\beta_0 = \beta_4 = 1\\ \beta_1 = \beta_3 = 4\\ \beta_2 = 6\end{cases} \tag{24}$$

Solving for the Euler Characteristic we find:

$$\chi(T^4) = \chi(T^2) \times \chi(T^2) = 0 \times 0 = 0 \tag{25}$$

All tori of any dimension, T^N, will have an Euler Characteristic of 0, because a fundamental multiple of all tori is a simple circle, S^1, with an Euler Characteristic of zero. Table 3 shows the products, in terms of Betti numbers, of some one and two-dimensional compact spaces.

Table 3: Betti Number Multiplication Table

	S^1	S^2	T^2
S^1	1,2,1	1,1,1,1	1,3,3,1
S^2	1,1,1,1	1,0,2,0,1	1,2,2,2,1
T^2	1,3,3,1	1,2,2,2,1	1,4,6,4,1
E^2	1,1,1,1	1,0,2,0,1	1,2,2,2,1
D^2	1,2,2,1	1,1,2,1,1	1,3,4,3,1
P^2	1,2,1,0	1,1,1,1,0	1,3,3,1,0
K^2	1,3,2,0	1,2,1,2,0	1,4,5,2,0
M^2	1,2,1,0	1,1,1,1,0	1,3,3,1,0

General Expression of Topology and Anisotropy

The fundamental goal of this work is to explicitly display the connection between the topology of the universe and the underlying empirical signature of that topology as indicated by anisotropies in the cosmic microwave background radiation. Betti numbers, and their associated topological invariants, will be used to provide a description of the topology of the universe. The space spanned by the Betti numbers will then be combined in a simple expression with the characterization of the anisotropies using the Sachs-Wolfe effect. An ideal representation would be a single expression that accepts the Betti numbers that specify a certain topology and the parameters that define the cosmological model to be tested. Such parameters include[17]: the density of matter, the density of radiation, the value of H_o, and the local spatial curvature, k. A term must also be added that explains the local geometry of the surface, and this comes from general relativistic terms $g_{\mu\nu}$. The Betti numbers contains 4 values in three dimensions, $g_{\mu\nu}$ contains 10 values, and the other terms contain one number each. This means the equation would be some space in 18 dimensions and would be incredibly difficult to solve. By symmetry, the 10 $g_{\mu\nu}$ terms simplify to only four, all of which are related to the radius of the universe. The radius of the universe information is contained in H_o, and can be left out of the equation.

There are a variety of ways to look for topological variations in the equations that actually describe the dynamics of the universe. Unfortunately the most direct and obvious method, using the Einstein field equations, does not yield any global topological information beyond the specification of a set of initial conditions in the early universe [18,19]. Newer more speculative theories, such as superstring theory and Ashtekar loop space, allow for topological change but until they are developed further, they will not connect directly with the current data. It is also necessary to assume that the large-scale global topology of the universe has not changed over time since the period of recombination [20](small-scale changes are expected, i.e. wormholes, etc.).

In 1967, Sachs and Wolfe were able to show that large scale fluctuations in the cosmic background radiation temperature as a function of position across the sky provides a way to measure the large scale fluctuations in the cosmological mass distribution in the standard cosmological model. These fluctuations from the nearly homogenous mass distribution can be seen in terms of Newtonian gravitational potential [21]. Small fluctuations in mass density in the early universe would have created gravitational potential. As photons passed through this change in gravitational potential they were redshifted. Because redshifted photons have less energy, they would show up today as temperature fluctuations in these early photons.

Imagine a path that traces back to the early universe at a very high red-shift where the mass density contrast averaged over some commoving (expanding with the universe) scale x is $\delta\rho/\rho=\delta_x$. The Newtonian gravitational potential energy caused by this fluctuation is [18]:

$$\phi \sim \frac{G\,\delta M}{ax} = \frac{G}{ax}\frac{\delta M}{M}\frac{4}{3}\pi\rho_b\,(ax)^3 \qquad (26)$$

$$= \frac{1}{2}\Omega H^2\,(ax)^2\,\delta_x \qquad (27)$$

The expansion rate scales as $H \propto a^{-3/2}$ in the Einstein-de Sitter limit, and the density difference goes as $\delta M / M = \delta_x \propto a(t)$. This means that the gravitational potential ϕ from the mass fluctuation is independent of time. The only way for the radiation to reach us is to first escape from the potential, which causes a gravitational redshift, $\delta\nu / \nu \sim \phi$. This will also cause a change in the cosmic microwave background temperature. The CMB anisotropy that is caused by the mass density fluctuation on a comoving scale x at the Hubble distance is given by [18]

$$\frac{\delta T}{T} \sim (H_0 a_0 x)^2\,\delta_x(0) \qquad (28)$$

A more detailed calculation carried out by Sachs and Wolfe goes as

$$\frac{\delta T(\theta,\phi)}{T} = \frac{1}{3}\Phi(\eta_{sls}, r_{sls}, \theta, \phi) + 2\int_{\eta_{sls}}^{\eta_0}\Phi'(\eta, r, \theta, \phi)d\eta. \qquad (29)$$

The first term in equation 29 is the direct Sachs Wolfe effect and the second term is the integrated Sachs Wolfe effect which describes the topology of all non-trivial spaces. Here η represents conformal time, η_0 is the present conformal time, η_{sls} is the conformal time at recombination (from the surface of last scattering), and $\Phi' = \delta\Phi$. The change in potential from recombination to the present day can be represented by [22]

$$\Phi''+3H(1+c_s^2)\Phi'-c_s^2\nabla\Phi+(2H'+(1+c_s^2)H)\Phi=0 \quad (30)$$

where H is the conformal Hubble factor and c_s is the speed of sound compared to the speed of light in the cosmological fluid. If the universe is flat, we have $c_s = 0$, $H = 2/\eta$ and $\Phi' = 0$. Because of this, the integrated Sachs Wolfe effect in equation 29 vanishes and the temperature fluctuations are all described by the first term. The presence of either a cosmological constant or curvature will cause the decay of the potential, Φ, and consequently a decay in the first term and the integral becomes the important term.

Because the cosmic microwave background data is taken in all directions from our sky, it can be represented as a two dimensional sphere. This skymap can be modeled as an angular power spectrum, which is shown as an expansion in spherical harmonics. The multipole expansion of the sky temperature as a function of angular position has the form [4]

$$\frac{\delta T}{T}(n) = \sum_{l,m} a_l^m Y_l^m(n) \tag{31}$$

$$a_l^m = -2\pi i^l \frac{H_0^2}{c^2} \sum_k \frac{\delta_x}{k^2} j_l(ky) Y_l^m(n) \tag{32}$$

where j_l is the lth order spherical Bessel function.

The third part of the general equation is related to the spatial curvature. The interesting properties of the curvature are indicated by its sign, k = -1, 0, +1. Spacetime can be considered flat if k is zero. If k is negative that implies a negative curvature, as in a compact hyperbolic manifold. This curvature parameter can be easily added to the general equation using the following function[1]

$$\begin{cases} S_k(X) = \sinh(X) & \text{if } k = -1 \\ S_k(X) = (X) & \text{if } k = 0 \\ S_k(X) = \sin(X) & \text{if } k = 1 \end{cases} \tag{33}$$

A general function that can describe the CMB anisotropies can be composed of only the discreet Betti number space, T(β), and the anisotropy information, F, which will contain the term $S_k(X)$, taken as a direct product. This results in

$$\Psi(\beta, \Omega, \Lambda, H_0, k) = T(\beta) F(\Omega, \Lambda, H_0, k) = \begin{pmatrix} \beta_0 \\ \beta_1 \\ \beta_2 \\ \beta_3 \end{pmatrix} F \tag{34}$$

One would not expect any coupling between these two spaces, since the local differential equations do not contain any topological information.

Finite Flat Models

There has been extensive study of the six possible flat, orientable, compact topologies for the universe. These six cases have received so much attention because they can be solved analytically. The mode functions can be analytically obtained which makes the solution for the angular power spectrum straightforward. Because of this, the second term from the Sachs-Wolfe effect equals zero.

$$\frac{\delta T(\theta,\phi)}{T} = \frac{1}{3}\Phi(\eta_{sls}, r_{sls}, \theta, \phi) + 2\int_{\eta_{sls}}^{\eta_0} \Phi'(\eta, r, \theta, \phi) d\eta \quad (35)$$

This leaves only [4]

$$\frac{\delta T(\theta,\phi)}{T} = \frac{1}{3}\Phi(\eta_{sls}, r_{sls}, \theta, \phi) \quad (36)$$

where $\Delta\eta = \int dt/a(t)$ is the conformal time between today and recombination. The potential for a compact manifold, Φ, can be thought of in terms of an eigenmode expression

$$\Phi = \int_{-\infty}^{\infty} d^3k \Phi_k \exp(i\Delta\eta\vec{k} \bullet \hat{n}) . \quad (37)$$

So the expression for $\delta T/T$ becomes

$$\frac{\delta T}{T}(n) = \sum \Phi_k \exp(i\Delta\eta\vec{k} \bullet \hat{n}) . \quad (38)$$

By identifying the value of Φ in terms of the three directions of k (k_x, k_y, k_z) the equation can be exactly solved.

If the temperature fluctuations are adiabatic, the Sachs-Wolfe relationship can be solved as a series [4]

$$\frac{\delta T}{T}(n) = -\frac{H_0^2}{c^2}\sum_k \frac{\delta_x \exp(iy\vec{k} \bullet \hat{n})}{k^2} \tag{39}$$

where y is the radius of the decoupling sphere, given by $y = 2c/H_0$, n describes a direction in the sky, δ_k is the density fluctuation in Fourier space and the sum is on wave numbers *k*. To simplify the equation, a rotationally invariant coefficient can be defined as [18]

$$a_l^2 = \sum_m \frac{|a_{lm}|^2}{(2l+1)}. \tag{40}$$

This implies the average *l*th multipole of the temperature fluctuation is given by

$$\left\langle a_l^2 \right\rangle = 16\pi \sum_k \frac{|\delta_x|^2 j_l^2(ky)}{(ky)^4}. \tag{41}$$

If the universe being modeled is simply connected, it has a positive curvature. There is only one possible topology, three-dimensional sphere, S^3. All wave vectors are allowed, and the sum can be switched to an integral, which gives [24]

$$\left\langle a_l^2 \right\rangle = \left\langle a_2^2 \right\rangle \frac{\Gamma(l+(n-1)/2)\Gamma((9-n)/2)}{\Gamma(l+(5-n)/2)\Gamma((3+n)2)}. \tag{42}$$

In a multiply connected universe, the simplest of which is the torus, T^3, not all wave vectors are allowed as they can wrap around the surface and interfere with themselves. For a torodial universe, only integral multiples of some wave vector are allowed along each of the three axes [5]. The space can easily be modeled using a parallelepiped tiling as shown below (FIGURE 19).

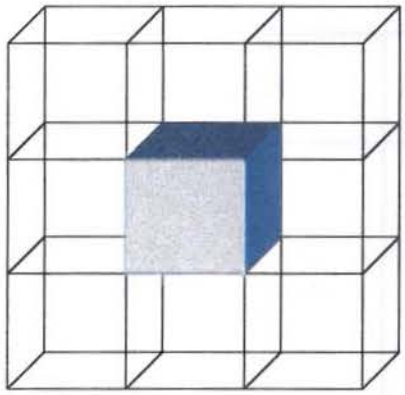

Figure 19: Tiling Flat Space With parallelepipeds

This shape is built on the parallelepiped by identifying: $x \rightarrow x + h$, $y \rightarrow y + b$, $z \rightarrow z + c$. By identifying the shape in this way, the eigen value is restricted to the following:

$$k_x = \frac{2\pi}{h} j,\ k_y = \frac{2\pi}{b} w,\ k_z = \frac{2\pi}{c} n \qquad (43)$$

The sum from the Sachs- Wolfe equation cannot be changed to an integral, because not all wave functions exist, therefore, it must be completed along each of the three axes as shown.

$$\left\langle a_l^2 \right\rangle = \sum_{p_x}\sum_{p_y}\sum_{p_z}\left(\frac{L}{2\pi yp}\right)^3 j_l^2\left(\frac{2\pi yp}{L}\right). \qquad (44)$$

There are three other compact flat topologies that can be modeled using the parallelepiped. Their triangulation and gravitational potential values, Φ, are shown in table 4.

Table 4: Flat Compact Parallelepiped Topologies [6]

SHAPE	EIGENMODES	Φ
Opposite faces identified	$k_x = k_y = k_z = \frac{2\pi}{h} j,$	$\Phi_{jwn} = \Phi_{jwn} e^{i\pi n}$
Opposite faces identified, with one pair rotated through an angle π	$k_x = \frac{2\pi}{h} j, k_y = \frac{2\pi}{b} w,$ $k_z = \frac{\pi}{c} n$	$\Phi_{jwn} = \Phi_{-j-wn} e^{i\pi n}$
Opposite faces identified, with one pair rotated through an angle $\pi/2$	$k_x = \frac{2\pi}{h} j, k_y = \frac{2\pi}{b} w,$ $k_z = \frac{\pi}{2c} n$	$\Phi_{jwn} = \Phi_{j-wn} e^{in\pi/2}$
First rotate about x by π, then rotate about y by π, then rotate about z by π.	$k_x = \frac{\pi}{h} j, k_y = \frac{\pi}{b} w,$ $k_z = \frac{\pi}{c} n$	$\Phi_{jwn} = \Phi_{-j-wn} e^{i\pi(j+w+n)}$

A correlation function can also be created that relates two points in the sky, **n** and **n'**, commonly called C_l. C_l represents the angular power spectrum. This correlation function is defined as [6]

$$C_l(\hat{n},\hat{n}') = \left\langle \frac{\delta T}{T}(\hat{n}) \frac{\delta T}{T}(\hat{n}') \right\rangle. \tag{45}$$

The previous table is expanded to include C_l's for each of the cases in Table 5.

Table 5: C_l Values for Flat Compact Parallelepiped Topologies

SHAPE	C_l
Opposite faces identified	$C_l \propto \sum_{jwn} \frac{P(k)}{k^3} j_l(\Delta\eta k)^2$
Opposite faces identified, with one pair rotated through an angle π	$C_l \propto \sum_{jwn} \frac{P(k)}{k^3} \frac{j_l(\Delta\eta k)^2}{2l+1} \sum_{m=-l}^{l} \left\lvert Y_{l,m}(\hat{k}) \right\rvert^2 (1+e^{i\pi(m+m)})$
Opposite faces identified, with one pair rotated through an angle $\pi/2$	$C_l \propto \sum_{jwn} \frac{P(k)}{k^3} \frac{j_l(\Delta\eta k)^2}{2l+1} \sum_{m=-l}^{l} \left\lvert Y_{l,m}(\hat{k}) \right\rvert^2 (1+e^{i(n+m)\pi/2}+e^{i(n+m)\pi}+e^{i(n+m)3\pi/2})$
First rotate about x by π, then rotate about y by π, then rotate about z by π.	$C_l \propto \sum_{jwn} \frac{P(k)}{k^3} \frac{j_l(\Delta\eta k)^2}{2l+1} \sum_{m=-l}^{l} \left\lvert Y_{l,m}(\hat{k}) \right\rvert^2 (1+e^{i(n+m)\pi/2}+e^{i(n+m)\pi}+e^{i(n+m)3\pi/2})$

There are two other compact, orientable, flat spaces that cannot be created from a parallelepiped tiling [6]. To model these shapes, a hexagonal tiling is required, as shown in Figure 20

Figure 20: Hexagonal tiling

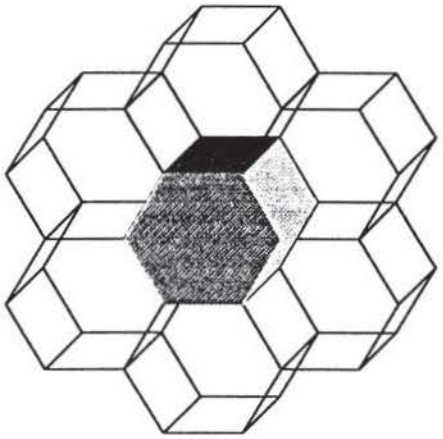

The three pairs of opposite sides of the hexagon are identified with each other. The face of the hexagon undergoes a rotation of $2\pi/3$ in one case and $\pi/3$ in the later. The eigenmodes and gravitational

Table 6: Flat Compact Hexagonal Topologies

SHAPE	EIGENMODES	Φ
Opposite sides of hexagon identified, face rotated at an angle of $2\pi/3$	$k_x = \frac{2\pi(n_2+n_3)}{h}$, $k_y = \frac{(n_2+n_2)}{b}$, $k_z = \frac{n_z}{3c}$	$\Phi = \Phi_{n_2 n_3 n_z} e^{ikz} \times \exp\left[i\frac{2\pi}{h}\left[n_2(x - \frac{1}{\sqrt{3}}y) + n_3(x + \frac{1}{\sqrt{3}}y) \right] \right]$
Opposite sides of hexagon identified, face rotated at an angle of $\pi/3$	$k_x = \frac{2\pi(n_2+n_3)}{h}$, $k_y = \frac{(n_2+n_2)}{b}$, $k_z = \frac{n_z}{6c}$	$\Phi = \Phi_{n_2 n_3 n_z} e^{ikz} \times \exp\left[i\frac{2\pi}{h}\left[n_2(x - \frac{1}{\sqrt{3}}y) + n_3(x + \frac{1}{\sqrt{3}}y) \right] \right]$

potential are given in Table 6. The values for the angular power spectrum are given in Table 7.

Table 7: C_l Values for Flat Compact Hexagonal Topologies

SHAPE	C_l
Opposite sides of hexagon identified, face rotated at an angle of $2\pi/3$	$C_l \propto \sum_{jwn} \frac{P(k)}{k^3} \frac{j_l(\Delta\eta k)^2}{2l+1} \sum_{m=-l}^{l} \left\|Y_{l,m}(\hat{k})\right\|^2$ $(1+e^{i(n_z+m)2\pi/3}+e^{i(n_z+m)4\pi/3})$
Opposite sides of hexagon identified, face rotated at an angle of $\pi/3$	$C_l \propto \sum_{jwn} \frac{P(k)}{k^3} \frac{j_l(\Delta\eta k)^2}{2l+1} \sum_{m=-l}^{l} \left\|Y_{l,m}(\hat{k})\right\|^2$ $(1+e^{i(n_z+m)\pi/3}+e^{i(n_z+m)2\pi/3}+e^{i(n_z+m)\pi}$ $+e^{i(n_z+m)4\pi/3}+e^{i(n_z+m)5\pi/3})$

Compact Hyperbolic Spaces

The mode functions for the flat models can be analytically obtained, on the other hand, no closed analytic expression of the eigenmodes is known for compact hyperbolic spaces. Therefore, the analysis of the CMB anisotropy in compact hyperbolic models has been considered very difficult. To overcome the difficulty, Inoue [9] proposed a numerical approach he called the direct boundary element method (DBEM) for computing the eigenmodes of the Laplace-Beltrami operator. Inoue has found that the expansion coefficients behave as if they were random Gaussian numbers. The angular power spectrum for some compact hyperbolic shapes can be obtained using this approach.

Temperature fluctuations in a multiply-connected cosmological model can be written as linear combinations of independent components of temperature correlations in a simply connected cosmological model. Assuming the initial fluctuations are random Gaussian, perturbations are adiabatic and super-horizon scalar type, the two-point temperature correlation in a compact hyperbolic cosmological model is written as [8]

$$\left\langle \frac{\delta T}{T}(n)\frac{\delta T}{T}(n')\right\rangle = \sum_{l,m,l',m'} \left\langle a_{lm}\, a^{*}_{l'm'}\right\rangle Y_{lm}(n) Y^{*}_{l'm'}(n) \tag{46}$$

$$= \sum_{\nu,\nu',l,m,l',m'} \left\langle \Phi_{\nu}\Phi_{\nu'}\right\rangle \xi_{\nu lm}\xi^{*}_{\nu' l'm'} L_{\nu lm} L^{*}_{\nu' l'm'}, \tag{47}$$

where

$$\langle \Phi_\nu \Phi_{\nu'} \rangle = \frac{4\pi^4 \mathrm{P}_\Phi(\nu)}{\nu(\nu^2+1)Vol(\Omega)} \delta_{\nu\nu'}, \tag{48}$$

$P_\Phi(\nu)$ is the initial power spectrum, $Vol(\Omega)$ is the volume of the fundamental domain found using the program Snappea [16], η_* is the conformal time at decoupling and η_0 is the conformal time at the present.

$$L_{\nu lm}(\eta_0, n) \equiv Y_{lm}(n) F_{\nu l}(\eta_0), \tag{49}$$

$$F_{\nu l}(\eta_0) \equiv \frac{1}{3}\Phi_t(\eta_*) X_{\nu l}(\eta_0 \eta_*) + 2\int_{\eta_*}^{\eta_0} d\eta \frac{d\Phi_t}{d\eta} X_{\nu l}(\eta_0 \eta), \tag{50}$$

$$\Phi_t(\eta) = \frac{5(\sinh^2 \eta - 3\eta \sinh \eta + 4\cosh \eta - 4)}{(\cosh \eta - 1)^3}. \tag{51}$$

Using these terms, a formula for the angular spectrum can be created [9]

$$(2l+1)\widetilde{C}_l = \sum_{m=l}^{l} \left\langle |a_{lm}|^2 \right\rangle$$

(52)

$$= \sum_{\nu,m} \frac{4\pi^4 P_\Phi(\nu)}{\nu(\nu^2+1)Vol(\Omega)} |\xi_{\nu lm}|^2 |F_{\nu l}|^2. \tag{53}$$

It is Inoue's assertion that for the 14 eigenmodes he calculated, the expansion coefficient, $\xi_{\nu lm}$ value will behave as random Gaussian

numbers [10]. This assumption works very well on almost all parts of the fundamental domain. These random numbers will not give the correct value if the point tested is very near a boundary or punctue in the space. This allows one an approximate method for computing the angular power spectrum. Only solutions for two such spaces have been attempted, the smallest Thurston manifold and the smallest Weeks manifold.

We have extended Inoue's work further by creating a method for calculating the large l values of the of the angular power spectrum for compact hyperbolic manifolds. The eigenmode expansion function, $X_{\nu l}$, from equation (50) can be replaced with the more general pFq Hypergeometric function as shown in equation (54)

$$F_{\nu l}(\eta_0) \equiv \frac{1}{3}\Phi_t(\eta_*)\,{}_pF_q + 2\int_{\eta_*}^{\eta_0} d\eta \frac{d\Phi_t}{d\eta}\,{}_pF_q, \tag{54}$$

A very large class of twice differentiable functions that are oscillatory can be expressed as ${}_pF_q$ functions. The general form of a ${}_pF_q$ function [24] is given in equation (55).

$${}_pF_q(\alpha;\beta;x) = \sum_{k=0}^{\infty} \frac{(\alpha_1)_k \ldots (\alpha_p)_k}{(\beta_1)_k \ldots (\beta_q)_k} \frac{x^k}{k!} \tag{55}$$

Where $(\alpha)_k$ is the Pochhammer function [26],

$$(\alpha)_k = \alpha(\alpha+1)(\alpha+2)\ldots(\alpha+k-1) = \frac{(\alpha+k-1)!}{(\alpha-1)!}. \tag{56}$$

For example, the ${}_pF_q$ function when p = 2 and q = 1 would be [25]

$$ {}_2F_1(\alpha_1,\alpha_2;\beta;x) = \sum_{k=0}^{\infty} \frac{(\alpha_1)_k (\alpha_2)_k}{(\beta_1)_k} \frac{x^k}{k!} \tag{57} $$

The ${}_pF_q$ function is a sufficiently general function to capture anisotropies for nearly all compact hyperbolic manifold functions. Each new set of p and q will give a new function and most likely a new fundamental domain of a compact hyperbolic manifold. The sensitivity of the selection of the ${}_pF_q$ function to the C_l value is small for large l values because the error at the boundary is small compared to the number of waves that will fit across the fundamental domain. If the point of observation is not near a singular point or a boundary, the eigenmodes of many compact hyperbolic manifolds can be expressed as some combination of ${}_pF_q$ functions. We agree with Inoue that this is most likely true for an observer on the Earth.

Table 8 contains some common oscillatory functions represented as ${}_pF_q$ functions. Another special ${}_pF_q$ function occurs so frequently in CMB fluctuation calculations it should be included here is the special case where x is held constant at 1. [26]

$$ {}_2F_1(a,b;c;1) = \frac{\Gamma(c)\Gamma(c-a-b)}{\Gamma(c-a)\Gamma(c-b)} \tag{58} $$

Table 8: ${}_pF_q$ Representation of Common Oscillating Functions[26]

Type of Function	pFq Representation
Ultraspherical	$T_n^{\beta}(x)=\frac{(n+2\beta)!}{2^{\beta}n!\,\beta!}\,{}_2F_1\left(-n,n+2\beta+1;1+\beta;\frac{1-x}{2}\right)$
Legendre	$P_n(x)={}_2F_1\left(-n,n+1;1;\frac{1-x}{2}\right)$
Associated Legendre	$P_n^m(x)=\frac{(n+m)!(1-x^2)^{m/2}}{(n-m)!\quad 2^m m!}\,{}_2F_1\left(m-n,m+n+1;1+m;\frac{1-x}{2}\right)$
Chebyshev	$T_n(x)={}_2F_1\left(-n,n;\frac{1}{2};\frac{1-x}{2}\right)$
Bessel	$J_{\nu}(x)=\frac{e^{-ix}}{\nu!}\left(\frac{x}{2}\right)^{\nu}{}_1F_1\left(\nu+\frac{1}{2};2\nu+1;2ix\right)$
Spherical Bessel	$j_{\nu+1/2}(x)=\frac{e^{-ix}}{(\nu+3/2)!}\left(\frac{x}{2}\right)^{\nu+1/2}{}_1F_1\left(\nu+1;2\nu+2;2ix\right)$

Using this generalization, power spectrum graphs, C_l, can be created for high angular resolution or large l. Figure 21 was created using the Spherical Bessel case of the ${}_pF_q$ function at small values of l.

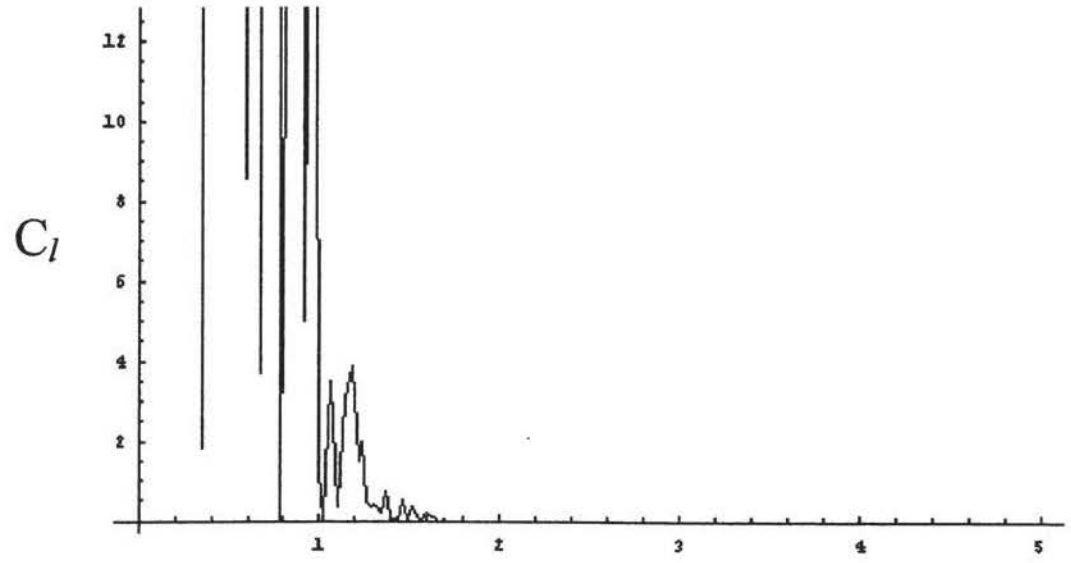

Figure 21: Spherical Bessel pFq Representation of the eigenmodes at small *l*.

There are peaks that represent structure as would be expected. The same graph can be represented at higher *l* values, shown in figure 22.

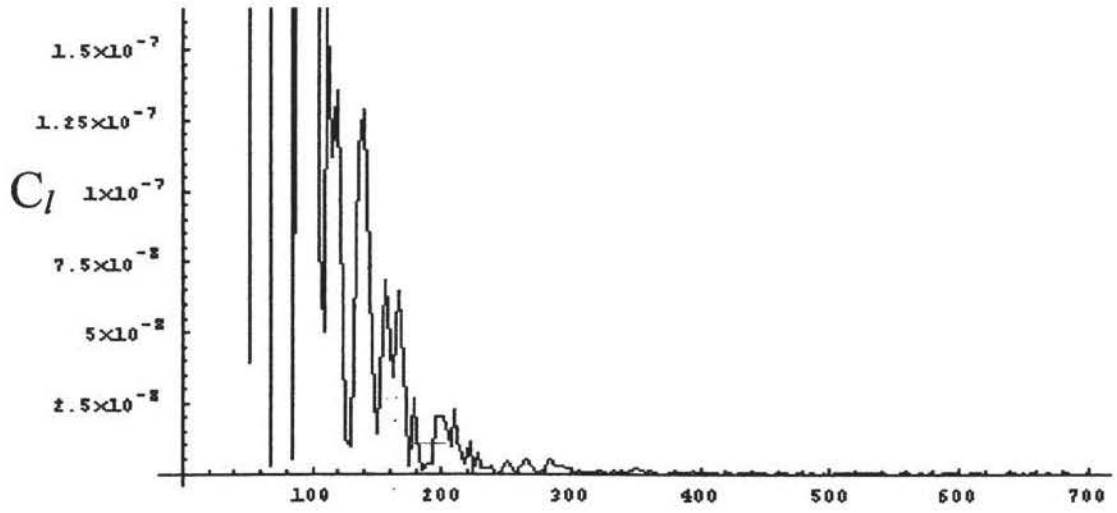

Figure 22: Spherical Bessel pFq Representation of the eigenmodes at large *l*

The peaks are still present, but the magnitude has become significantly lower. As long as the wavelength of the eigenmodes is small and there are many waves within the fundamental domain, their endpoints on the boundary become less important. This means the type of ${}_pF_q$ function used is not really important, many values of p and q will give a good approximation of the space.

More rigorous study will determine if the random Gaussian method is an acceptable replacement for the expansion coefficient. With the low resolution CMB data we currently have, the ${}_pF_q$ functions seem to be a good approximation, the major test of their validity will be the higher resolution of the MAP and PLANCK satellites. Until then, this method provides a powerful way to explore many compact hyperbolic manifolds without the complicated eigenmode calculation.

Angular Power Spectrum Plots

In this work we analyze temperature fluctuations in the cosmic background radiation for the simplest multiply connected topology, the three dimensional torus, T^3. The measurements are compared to a value l, which is equal to

$$l = \frac{180^\circ}{\Delta\theta}. \tag{54}$$

where θ equals the angular measure of the sky. A large value of l indicates a higher resolution. Because the perturbations depend on an unknown constant, the normalization of the power spectrum $|\delta_k|^2$, it is convenient to develop the data in terms of a ratio that eliminates the constant. The torus will be compared to the simply connected universe, S^3, by a ratio T^3/S^3. Eliminating the constant will eliminate a value of l, l=1. This is acceptable because l=1 corresponds to the dipole which can be attributed to the Earth's motion with respect to the universal cosmic background radiation. The power spectrum will be restricted to n=1 which is commonly accepted in the standard cosmological model.

The ratio of temperature fluctuations in between a torus, T^3, and a sphere, S^3, are shown in Figure 23. The various peaks in the graph would imply differences in the torodial shaped universe to the simply connected sphere universe. For the early values of l the temperature fluctuations seem to vanish. This is expected in a

cubically symmetric universe (Zel'dovich). The ratio of torus size to horizon size is 0.45.

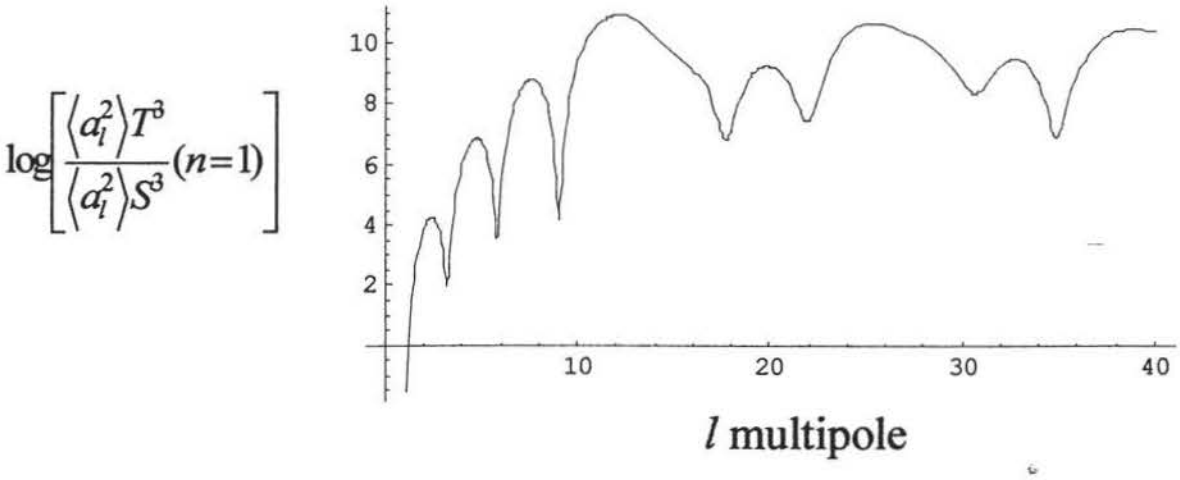

FIGURE 23: Power Spectrum, T^3/S^3, Torus smaller than horizon.

By simply altering the parameters of the equation, like the value of the Hubble constant, the size of the torus compared to the horizon, or the matter density, many different sizes and shapes of peaks can be created. This is demonstrated in Figure 24 and 25.

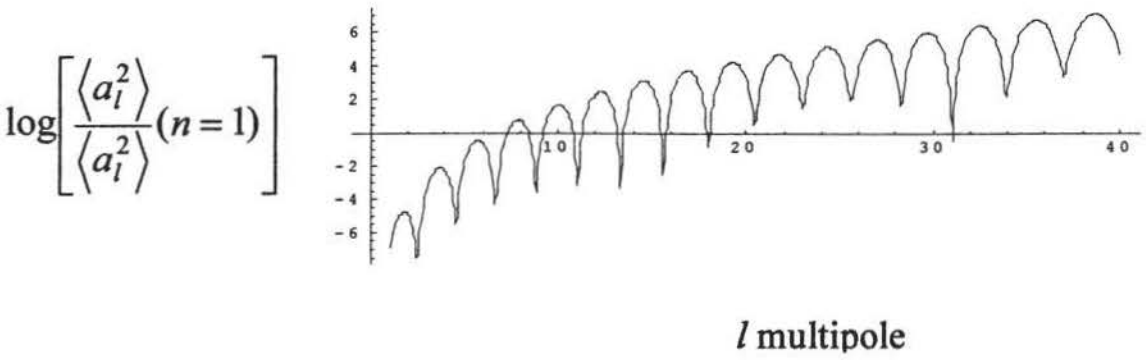

Figure 24: Power Spectrum, T^3/S^3, High Density

In Figure 24, the density is increased, and the pattern of the peaks becomes very sinusoidal.

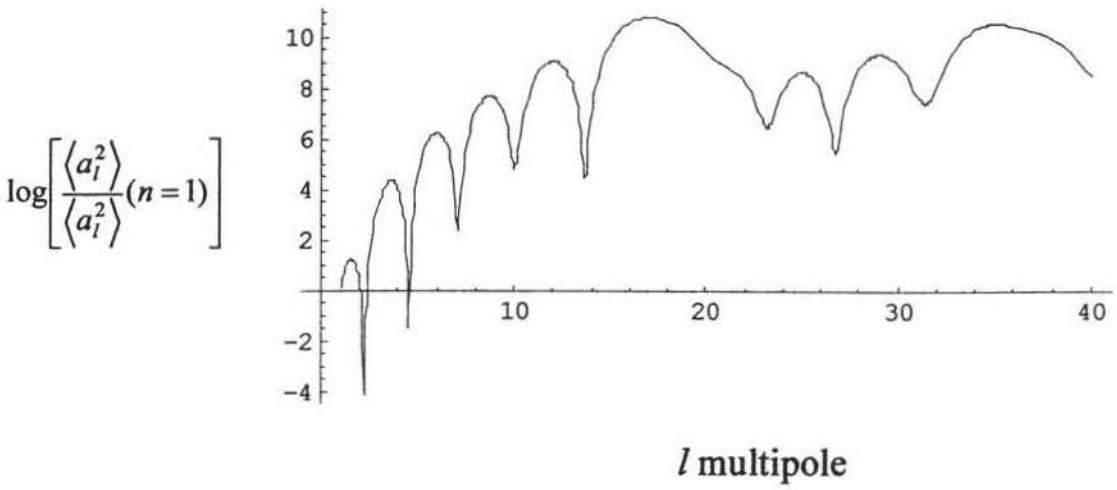

Figure 25: Power Spectrum, T^3/S^3, Small Density.

There is much interest in large values of l since the Boomerang data reported a peak at $l \sim 200$. Figure 26 compares the temperature fluctuations to $l = 600$. The size of the torus compared to the horizon is 0.05%. After $l = 100$, this graph is no longer interesting.

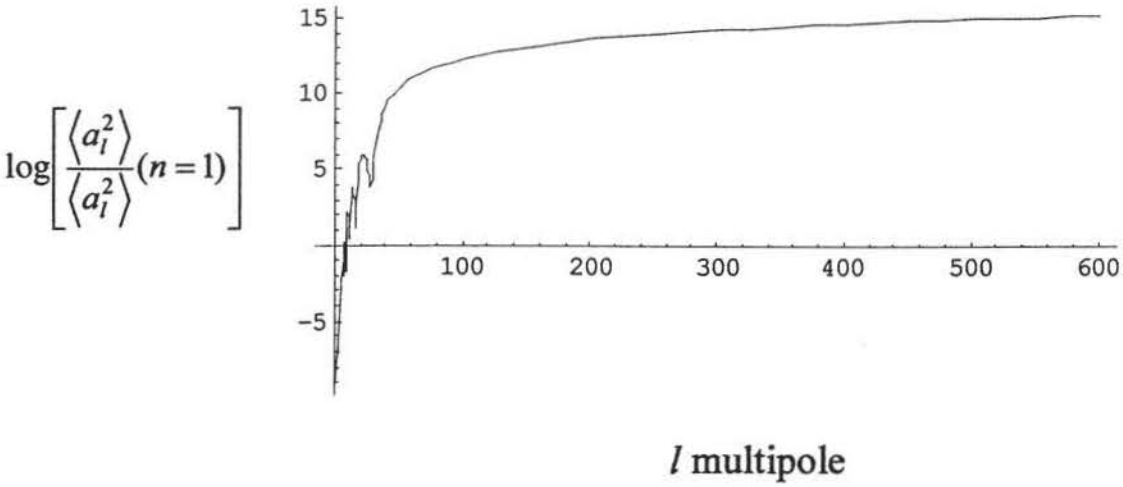

Figure 26: Power Spectrum, T^3/S^3, High Angular Resolution

A peak at large l values can be obtained by changing the constraints of the equation. The torus has been expanded to 0.25% of the size of the horizon in Figure 27. Because the position and height of the

peak can be adjusted almost any peak can be created assuming the right parameters.

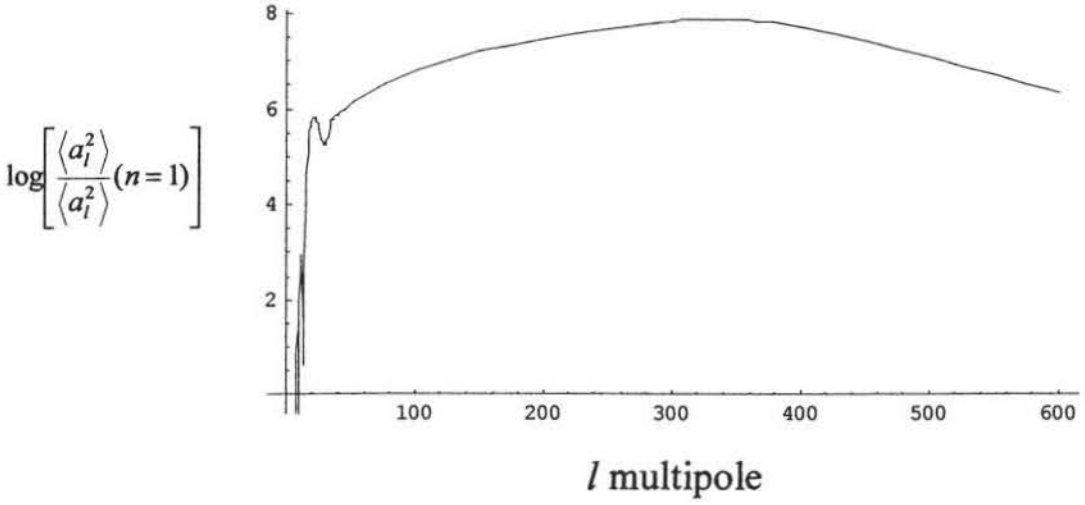

Figure 27: Power Spectrum, T^3/S^3, High Angular Resolution, High Density

A three dimensional graph can be created using the power spectrum ratio, the angular resolution (l multipole) and the probability of temperature fluctuation. These graphs contain a great amount of information. The difference between the sphere and torus becomes quite obvious, and complicated structure is quite evident. Just as with the two dimensional plots presented previously, the three dimensional plots are very sensitive to changes in the universal parameters.

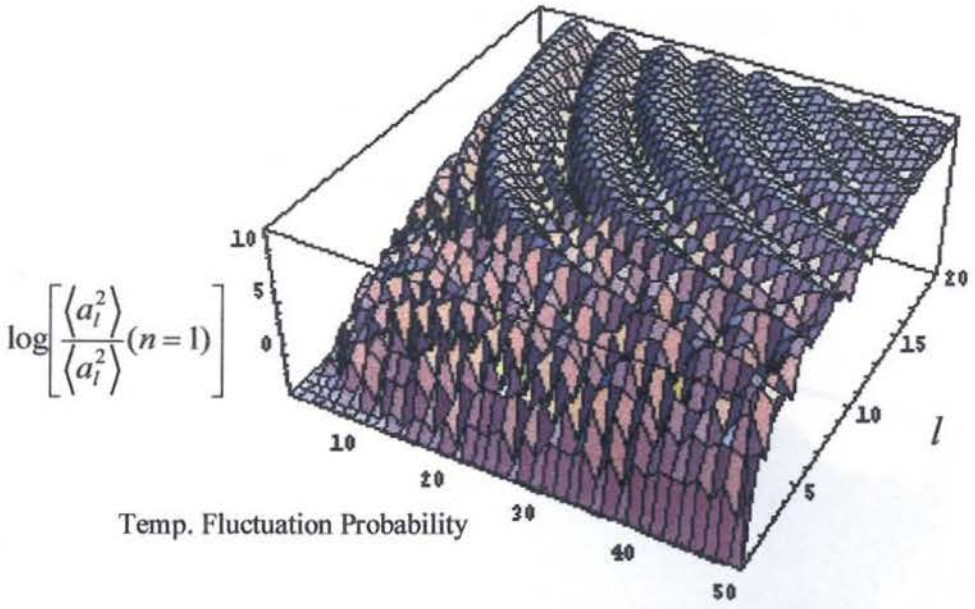

Figure 28: 3-D Power Spectrum, T^3/S^3, Torus smaller than the horizon.

Figure 28 shows the power spectrum for the same parameters as figure 23, only measuring to an l value of 20. The same relationship and parameters will also demonstrate fluctuations at high l as shown in figure 29.

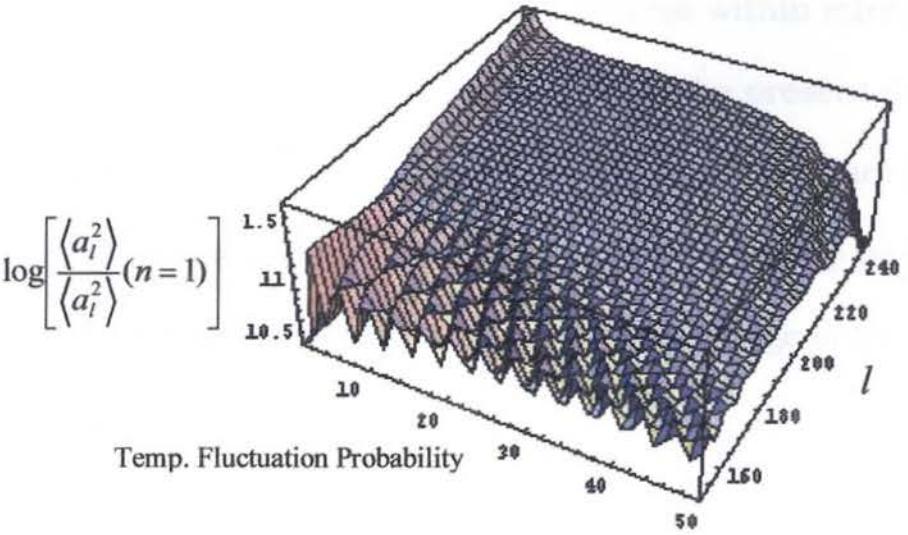

Figure 29: 3-D Power Spectrum, T^3/S^3, Torus smaller than the horizon, High angular resolution

By increasing the value of the Hubble constant used in the Figure 28 by 20% and keeping the other parameters constant, the ripples in the graph can be shifted to a higher l value as demonstrated in Figure 30.

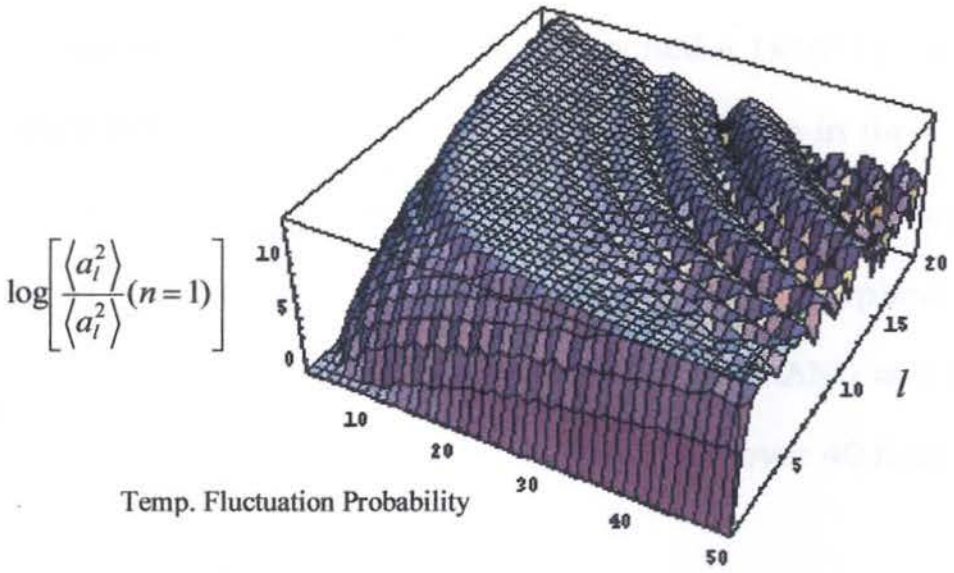

Figure 30: 3-D Power Spectrum, T^3/S^3, Torus smaller than the horizon, H_o increased by 20%

By altering the parameters of the universe within current accepted values, many shapes can be shown to fit the present data. This means that our present knowledge of the temperature fluctuations of the CMB is not accurate enough to eliminate many possibilities. The next section will describe our current knowledge of the data, and the future possibilities.

Boomerang

The measurement of the Cosmic Microwave Background radiation took a great leap forward on April 26, 2000. A project called Balloon Observations of Millimetric Extragalactic Radiation and Geophysics, or BOOMERANG, launched a $1x10^6$ m^3 balloon that carried a telescope above the Antarctic for 10 days in the winter of 1998 [18]. In order to make the extremely sensitive measurements, the balloon was lifted above 99% of the Earth's atmosphere to a height of approximately 37 kilometers. BOOMERANG was only able to map 2.5% of the sky, but its resolution was over 40 times that of the COBE satellite [20].

BOOMERANG images help to determine the geometry of space. By observing the characteristic size of hot and cold spots in the BOOMERANG images, the geometry of space can be determined. Cosmological simulations predict that if our universe has a flat geometry, (in which standard high school geometry applies), then the BOOMERANG images will be dominated by hot and cold spots of around 1 degree in size (bottom center). If, on the other hand, the geometry of space is curved, then the bending of light by this curvature of space will distort the images [19]. If the universe is closed, so that parallel lines converge, then the images will be magnified by this curvature, and structures will appear larger than 1 degree on the sky (bottom left). Conversely, if the universe is open,

and parallel lines diverge then structures in the images will appear smaller (bottom right). Comparison with the BOOMERANG image (top) indicates that space is nearly flat.

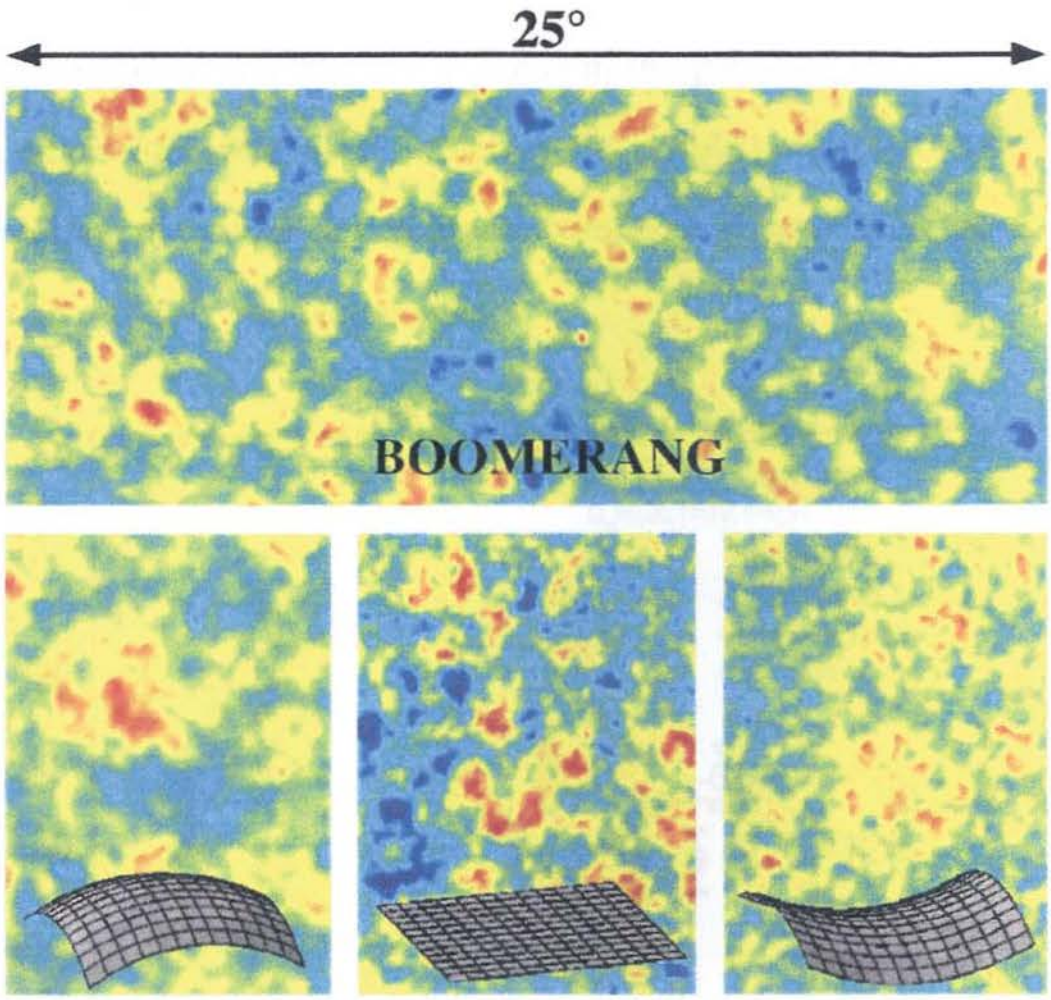

FIGURE 40 : [21]

The data from the Boomerang mission shows a strong peak at $l = 200$ (Figure 41). This is a peak at less than 1° angular resolution, which drops of steeply until $l = 400$. This steep drop is consistent with a structure predicted from acoustic oscillations in the adiabatic cold dark matter.[16] There is also evidence for one or more peaks

between $l = 200$ and $l = 1000$. These peaks are shorter than the peak at 200, but must also be explained. It was demonstrated in the previous chapter that peaks could be described in this l range by simply changing any of a number of cosmological parameters. The important point to notice is the peaks in the previous chapter were created on a torodial space, which is not simply connected. The Boomerang data does not eliminate complicated topological structure such as multiply connected spaces.

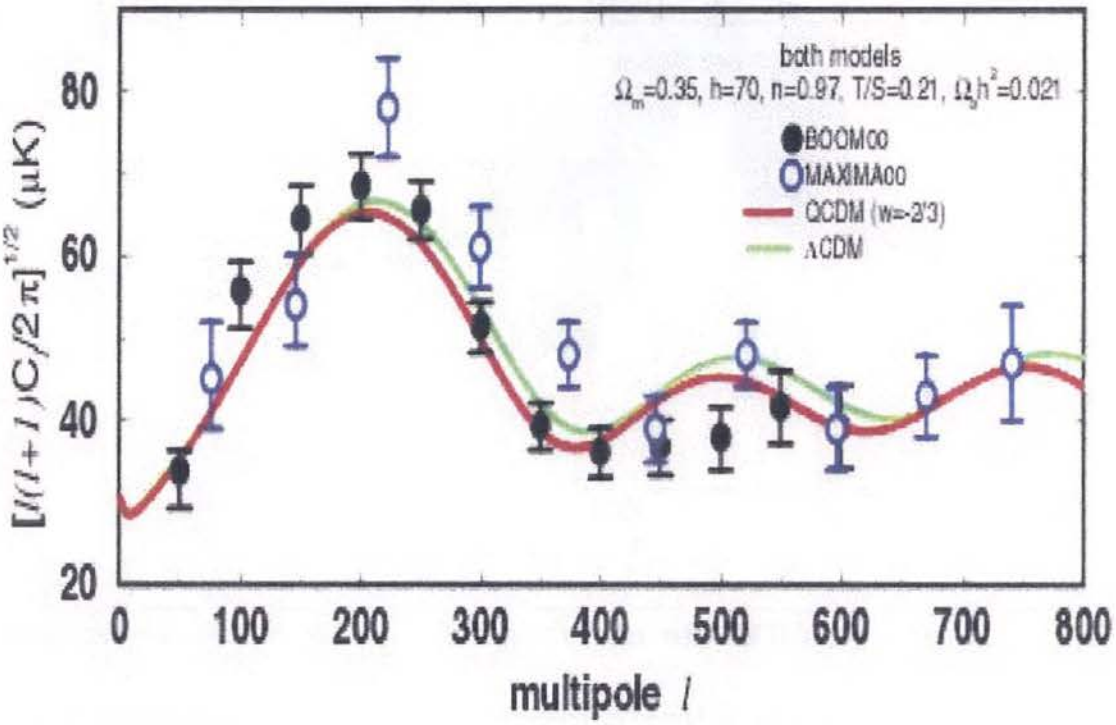

Figure 41: CMB Angular Power Spectra From Boomerang [21]

Many different groups have taken cosmic microwave background data, including the boomerang group, the COBE satellite and many other balloon-launched detectors. The complete total of this data is presented in figure 42. The high l values are obviously

not as explored as the small l's. This will change soon as the MAP and Planck satellites are due to be launched within the next five years.

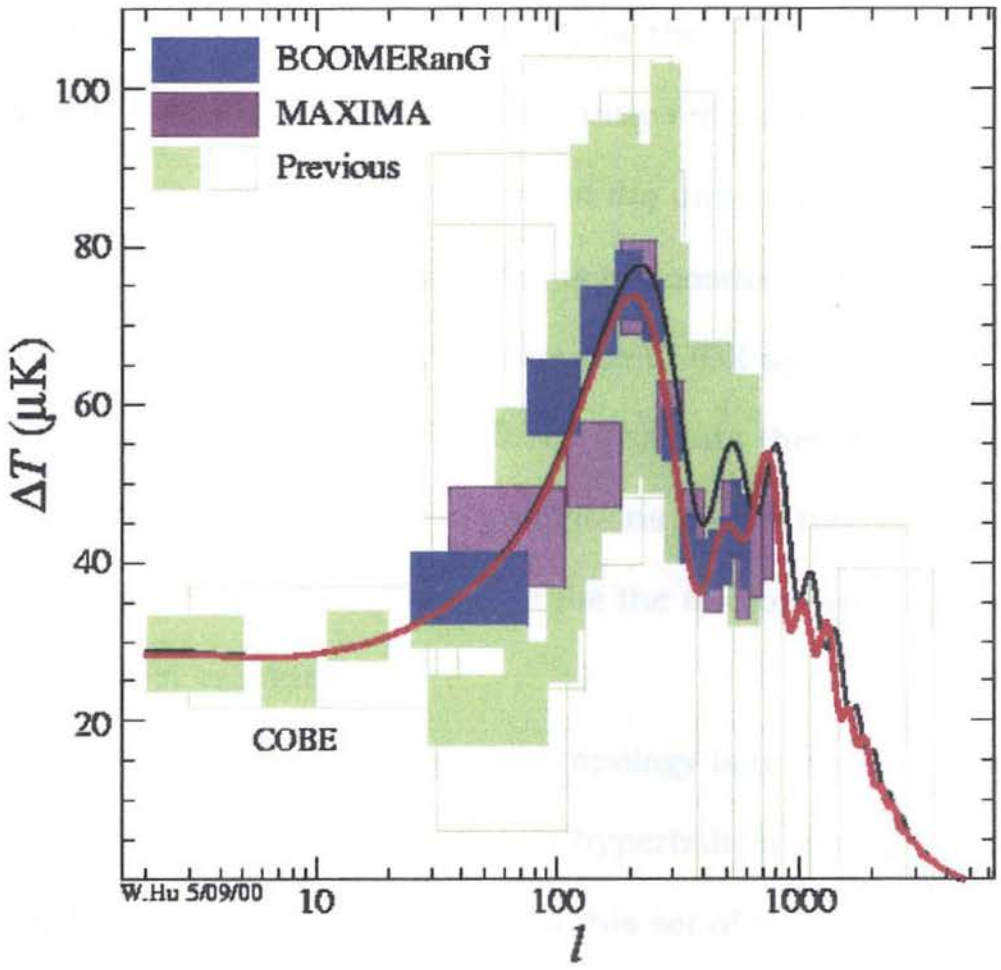

Figure 42: Angular Power Spectrum of CMB Anisotropies [12]

While COBE and Boomerang put considerable constraints on the topology of the universe, there are many things we cannot be sure of. The shape of the universe will remain a mystery until the cosmological parameters are known to greater uncertainty. Until then there are many combinations of parameters that can be used to describe the observed data.

Conclusion

The quest to determine the global topology of the universe is a celebrated and ancient question. In general the laws of physics that are differential are local and do not determine the shape. The last 50 years have seen an ever increasing and, for the most part converging, series of observations that have significantly reduced the number of possibilities associated with the shape of the universe. The most important topologically amongst these is the cosmic microwave background anisotropies collected from the COBE satellite and the BOOMERanG high atmosphere balloon. The data they provide is not accurate enough to make definite predictions on the topology. In the next decade, MAP and PLANCK will probe the microwave anisotropies to a much higher resolution.

The current goal of cosmological topology is to classify as many of the possible manifolds, flat, compact hyperbolic and positively curved, before the data comes in. With this set of manifolds classified, then build a set of CMB skymaps that match each possible shape. When MAP and PLANCK provide us with more accurate data, it will be easy to compare the data to the existing maps to find possible matches expanding our knowledge of the universe.

Bibliography

1. J.P. Luminet and B.F. Roukema, "Topology of the Universe: Theory and Observation," 1999, preprint (arXiv:astro-ph/9901364 v3)
2. K. Schwarzchild, *Class. Quant. Grav.*, **15,** 2539 (1998)
3. Einstein, *Postcard to Hermann Weyl*, June 1918, from Einstein Archives, Princeton
4. D. Stevens, D. Scott and J. Silk, "Microwave Background Anisotropy in a Torodial Universe," *Phys. Rev. Lett.*, **71,** 20 (1993)
5. J. Levin, E. Scannapieco, and J. Silk, "Is the Universe Infinite or is it Just Really Big?" *Phys. Rev. D*, **58,** 103516 (1998a)
6. J. Levin, E. Scannapieco, and J. Silk, "The Topology of the Universe: the Biggest Manifold of Them All," 1998, preprint (arXiv:gr-qc/9803036)
7. E. Scannapieco, J. Levin, and J. Silk, "Temperature Correlations in a Finite Universe," 1998, preprint (arXiv:astro-ph/9811226 v3)
8. K.T. Inoue and K. Tomita, "Temperature Correlations in a Compact Hyperbolic Universe," 1999, preprint (arXiv:astro-ph/9906304)

Bibliography

9. K.T. Inoue, "CMB Anisotropy in Compact Hyperbolic Universes," 1999, preprint (arXiv:astro-ph/9903446 v2)

10. K.T. Inoue, "Geometric Gaussianity and Non-Gaussianity in the Cosmic Microwave Background," 2000, preprint (arXiv:astro-ph/0002281 v2)

11. NASA website, The COBE homepage, http://space.gsfc.nasa.gov/astro/cobe/

12. Wayne Hu Website, *The Physics of Microwave Background Anisotropies,* Institute for Advanced Study, http://www.sns.ias.edu/~whu/physics/physics.html

13. J.R. Weeks, *The Shape of Space,* Marcel Dekker, INC, New York, NY, 1985

14. R.L. Bishop and S.L. Goldberg, *Tensor Analysis on Manifolds,* Dover Publications, New York, NY, 1968

15. M. Kaku, *Introduction to Superstrings and M-Theory,* Springer, New York, NY, 1998

16. J. R. Weeks, Snappea: *A computer program for creating and studying hyperbolic manifolds,* available at http://www.geom.umn.edu/software/download/snappea.html

17. J. Bernstien and G. Freiberg, *Cosmological Constants,* Colombia Univ. Press, NY, 1986

Bibliography

18. P.J.E. Peebles, *Principles of Physical Cosmology*, Princeton Univ. Press, Princeton, NJ, 1993

19. S.W. Hawking and G.F.R. Ellis, *The Large Scale Structure of Space-Time*, Cambridge Univ. Press, 1973

20. V. Rubin, G. Coyne, *Large Scale Motions in the Universe*, Princeton Press, NJ, 1988

21. I. Newton, *The Principia*, Translated by Andrew Motte, Prometheus Books, Amherst, NY, 1995

22. N.J. Cornish and D.N. Spergel, "A Small Universe After All?" 1999, preprint (arXiv:astro-ph/9906401 v2)

23. C.W. Misner, K.S. Thorne, J.A. Wheeler, *Gravitation*, W.H. Freeman and Company, San Francisco, CA, 1973

24. I.S. Gredshteyn and I.M. Ryzhik, *Table of Integrals Series and Products*, Academic Press, NY, 1965

25. J. Spanier and K.B. Oldham, *An Atlas of Functions*, Hemisphere Books, NY, 1987

26. G.B. Arfken and H.J Weber, *Mathematical Methods For Physicists*, Academic Press, New York, NY, 1995

27. P. de Bernardis, et al., "Mapping the CMB Sky: The Boomerang Experiment," 1999, preprint (arXiv:astro-ph/9911461)

Bibliography

28. P.D. Mauskopf, et al., "Measurement of a Peak in the CMB Power Spectrum from the North American Test Flight of Boomerang," 1999, preprint (arXiv:astro-ph/9911444)

Appendix A

Mathematica Code for the Power Spectrum of Compact Hyperbolic Manifolds at High l Using pFq Representations

```
alm := 4 Pi^4;
pn := 1;
u := 1.0;
Pk = u^pn;
epnu := Random[];
Vol := .96;
confto := 0.1;
conftf := 1.1;
Phi := 5 (Sinh[conftf] - 3 conftf Sinh[conftf] + 4 Cosh[conftf] - 4) / (Cosh[conftf] - 1)^3;
Fnul := {2 Pi / confto}^(.5) BesselJ[l + 0.5, confto];
Print[Fnul];
Coef := (alm Pk) (epnu)^2 / (Vol (2 l + 1));
Cl := Coef (Phi Fnul)^2;
Clg := Coef (Phi HypergeometricPFQRegularized[{2, 1}, {1}, l])^2;
Print[Cl, l];
Plot[Cl, {l, 0, 5}, PlotPoints -> 5];
Plot[Clg, {l, 2, 700}, PlotPoints -> 5];
```

Appendix B

Mathematica Code for the Three Dimensional Power Spectrum Plots of the Ratio Torus, T^3, to Sphere, S^3.

```
n := 1;
G1 = Gamma[x + (n - 1) / 2];
G2 = Gamma[(9 - n) / 2];
G3 = Gamma[x + (5 - n) / 2];
G4 = Gamma[(3 + n) 2];
ALN = (G1 G2) / (G3 G4);
ALN2 = ALN^2;
G5 = Log[ALN2];
G6 = Abs[G5];
y = 20;
L = 1;
a = 2 Pi;
vi = (a y i / (c L));
jl = (Pi / (2 vi))^(1 / 2) BesselJ[x + 1 / 2, vi];
ALT2 = Sum[(vi)^(-3) (jl^2), {i, 1, 20}];
RNT = Log[ALT2 / ALN2];
Plot3D[RNT, {x, 1, 50}, {c, .1, 20}, PlotPoints -> 40];
```